

3-Aminopyrrolidinone Farnesyltransferase Inhibitors: Design of Macrocytic Compounds with Improved Pharmacokinetics and Excellent Cell Potency

Ian M. Bell,^{*,†} Steven N. Gallicchio,[†] Marc Abrams,[‡] Lorena S. Beese,[§] Douglas C. Beshore,[†] Hema Bhimnathwala,[‡] Michael J. Bogusky,[†] Carolyn A. Buser,[‡] J. Christopher Culberson,^{||} Joseph Davide,[‡] Michelle Ellis-Hutchings,[‡] Christine Fernandes,[‡] Jackson B. Gibbs,[‡] Samuel L. Graham,[†] Kelly A. Hamilton,[‡] George D. Hartman,[†] David C. Heimbrook,[‡] Carl F. Homnick,[†] Hans E. Huber,[‡] Joel R. Huff,[†] Kelem Kassahun,[⊥] Kenneth S. Koblan,[‡] Nancy E. Kohl,[‡] Robert B. Lobell,[‡] Joseph J. Lynch, Jr.,[∇] Ronald Robinson,[‡] A. David Rodrigues,[⊥] Jeffrey S. Taylor,[§] Eileen S. Walsh,[‡] Theresa M. Williams,[†] and C. Blair Zartman[†]

Departments of Medicinal Chemistry, Cancer Research, Molecular Systems, Drug Metabolism, and Pharmacology, Merck Research Laboratories, West Point, Pennsylvania 19486, and Department of Biochemistry, Duke University Medical Center, Durham, North Carolina 27710

Received November 19, 2001

A series of macrocyclic 3-aminopyrrolidinone farnesyltransferase inhibitors (FTIs) has been synthesized. Compared with previously described linear 3-aminopyrrolidinone FTIs such as compound **1**, macrocycles such as **49** combined improved pharmacokinetic properties with a reduced potential for side effects. In dogs, oral bioavailability was good to excellent, and increases in plasma half-life were due to attenuated clearance. It was observed that in vivo clearance correlated with the flexibility of the molecules and this concept proved useful in the design of FTIs that exhibited low clearance, such as FTI **78**. X-ray crystal structures of compounds **49** and **66** complexed with farnesyltransferase (FTase)–farnesyl diphosphate (FPP) were determined, and they provide details of the key interactions in such ternary complexes. Optimization of this 3-aminopyrrolidinone series of compounds led to significant increases in potency, providing **83** and **85**, the most potent inhibitors of FTase in cells described to date.

Introduction

Interest in protein farnesyltransferase (FTase) inhibitors as potential therapeutic agents for the treatment of cancer was initiated by the observation that the protein product of the *ras* oncogene required farnesylation for biological function.^{1,2} Indeed, farnesyltransferase inhibitors (FTIs) have been shown to inhibit the growth of a variety of human tumor lines in cell culture and, more recently, to have clinical efficacy for the treatment of several cancers.³ Interestingly, the original hypothesis that FTIs would block Ras function has been invalidated by subsequent studies, and it is now generally acknowledged that the biological effects of FTIs must be due to the inhibition of farnesylation of other proteins.⁴ A number of groups have been pursuing FTIs, and a wide range of structural classes have been identified.^{3,5}

We have previously described the design of 3-aminopyrrolidinone-based inhibitors of FTase such as compound **1** (Figure 1) as part of an effort to develop orally active FTIs.⁶ While **1** displayed good oral bioavailability (*F* = 81% in dogs) and was a highly potent inhibitor of FTase in cell culture, it had a suboptimal plasma half-life (*t*_{1/2} = 1.1 h in dogs) and caused a 10% prolongation

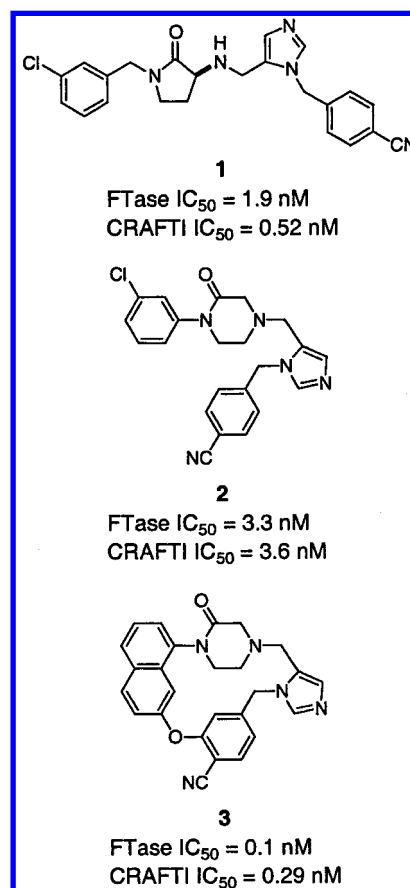


Figure 1. Aminopyrrolidinone and piperazinone farnesyltransferase inhibitors.

* To whom correspondence should be addressed at the Department of Medicinal Chemistry, Merck Research Laboratories, WP14-2, P.O. Box 4, West Point, PA 19486. Tel (215) 652-6455; fax (215) 652-7310; e-mail ian_bell@merck.com.

[†] Department of Medicinal Chemistry, Merck Research Laboratories.

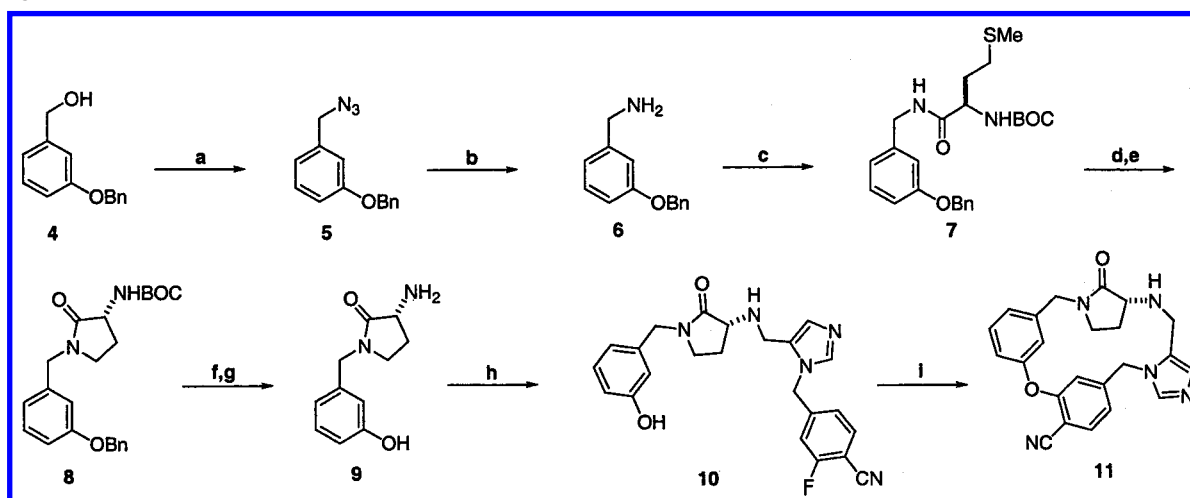
[‡] Department of Cancer Research, Merck Research Laboratories.

[§] Department of Biochemistry, Duke University Medical Center.

^{||} Department of Molecular Systems, Merck Research Laboratories.

[⊥] Department of Drug Metabolism, Merck Research Laboratories.

[∇] Department of Pharmacology, Merck Research Laboratories.

Scheme 1^a

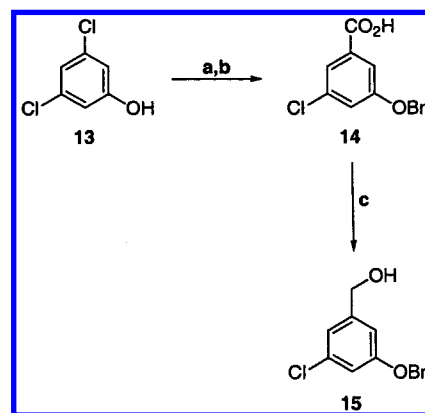
^a Reagents: (a) DPPA, DBU, toluene; (b) LiAlH_4 , THF; (c) (*R*)-BOC-methionine, PyBOP, DIEA, CH_2Cl_2 ; (d) MeI; (e) $\text{Li}(\text{Me}_3\text{Si})_2\text{N}$, THF; (f) H_2 , $\text{Pd}(\text{OH})_2$, HOAc, EtOH; (g) HCl, EtOAc; (h) 1-(4-cyano-3-fluorobenzyl)-5-imidazolecarboxaldehyde, DIEA, NaCNBH_3 , MeOH; (i) Cs_2CO_3 , DMF.

of the QT_c interval in dogs at a plasma level of $2.5 \mu\text{M}$.⁶ The latter observation was a concern because of the potential for causing cardiac arrhythmia in patients. Thus, our efforts became focused on the improvement of plasma half-life and on increasing the window between plasma levels that were projected to be efficacious and those that might cause undesirable cardiac effects.

In a related class of piperazinone-based FTIs, which includes the Merck clinical candidate **2**, macrocyclization afforded **3**, which possessed enhanced activity against FTase (Figure 1).⁷ On the basis of this observation, we decided to explore macrocyclic analogues of **1** in the hope that they would offer improved potency and an increased window between inhibition of FTase and prolongation of the QT_c interval in vivo. This report describes the evolution of aminopyrrolidinone **1** into compounds with improved pharmacokinetic properties, enhanced cell potency, and a reduced propensity to prolong the QT_c interval.

Chemical Methods

Scheme 1 describes the synthetic steps that were generally used for the construction of these macrocyclic FTIs, with compound **11** as an example. Commercially available 3-(benzyloxy)benzyl alcohol **4** was treated with DPPA and DBU to give azide **5**, which was reduced to amine **6** by LiAlH_4 . Coupling of **6** and (*R*)-BOC-methionine under PyBOP conditions and the eventual cyclization to form the pyrrolidinone **8** was accomplished as previously described.⁶ Standard removal of the protecting groups provided the aminopyrrolidinone **9** in high enantiomeric purity [enantiomeric excess (ee) > 98%] and reductive alkylation of **9** with 1-(4-cyano-3-fluorobenzyl)-5-imidazolecarboxaldehyde⁷ by use of NaCNBH_3 in MeOH gave phenol **10**. This phenol was subjected to Cs_2CO_3 in DMF at 50°C to afford the desired macrocycle **11** as well as a 14% yield of the corresponding dimeric macrocycle. Formation of dimeric byproduct was favored by the relatively high concentration of this macrocyclization (0.12 M). It was found that such oligomerization reactions could be largely avoided by performing the cyclizations at greater dilution and

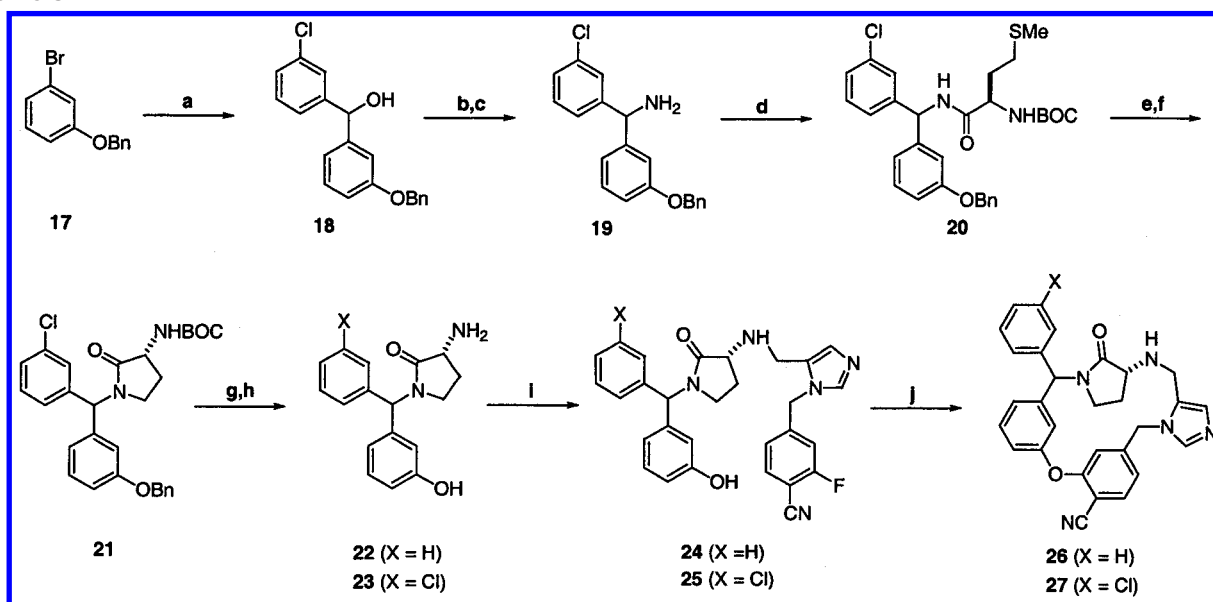
Scheme 2^a

^a Reagents: (a) Cs_2CO_3 , benzyl bromide, DMF; (b) Mg, CO_2 , Et_2O ; (c) LiAlH_4 , THF.

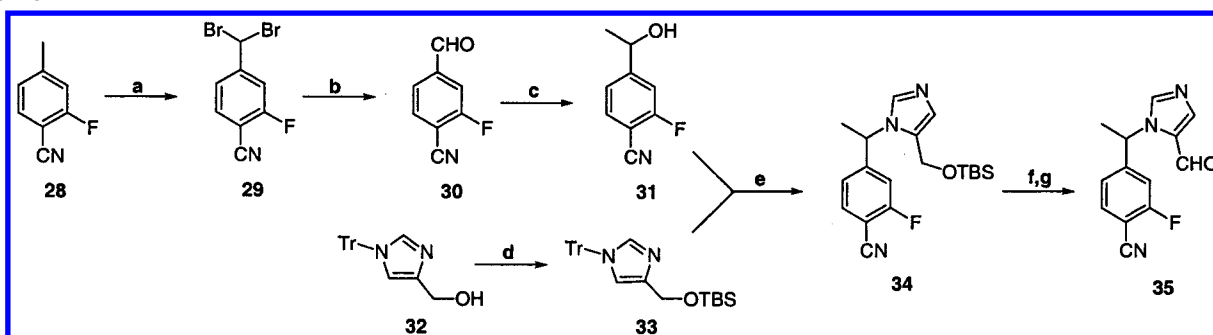
most subsequent examples were run at lower concentrations (0.005–0.01 M), as detailed in the Experimental Section.

Protection of 3,5-dichlorophenol **13** as the benzyl ether and treatment with Mg provided the Grignard reagent, which was quenched with carbon dioxide to give carboxylic acid **14**, as shown in Scheme 2. Reduction of **14** with LiAlH_4 in THF gave benzyl alcohol **15**, which was converted to the macrocycle **16** in analogy with alcohol **4** in Scheme 1.

The synthetic route to aryl-substituted macrocycles **26** and **27** is depicted in Scheme 3. Bromide **17** was reacted with Mg in THF to form the Grignard reagent, and this was treated with 3-chlorobenzaldehyde to give alcohol **18**, which was elaborated as described (vide supra) to produce **21** as a mixture of diastereomers (~1:1). After removal of the benzyl protecting group, silica gel chromatography allowed the separation of diastereomers. Deprotection of each diastereomer afforded compounds **23A** and **23B**. Reductive alkylation of **23A** followed by the standard macrocyclization step provided **27A**. Diastereomer **25B** failed to successfully macrocyclize under the Cs_2CO_3 conditions, producing only several byproducts. Use of KF on alumina and 18-crown-6 in acetonitrile as alternative, less-basic reaction conditions provided the desired macrocycle **27B**. Ex-

Scheme 3^a

^a Reagents: (a) (i) Mg, THF; (ii) *m*-chlorobenzaldehyde; (b) DPPA, DBU, toluene; (c) LiAlH₄, THF; (d) (*R*)-BOC-methionine, PyBOP, DIEA, CH₂Cl₂; (e) MeI; (f) Li(Me₃Si)₂N, THF; (g) H₂, Pd(OH)₂, HOAc, EtOAc, EtOH; (h) HCl, EtOAc; (i) 1-(4-cyano-3-fluorobenzyl)-5-imidazolecarboxaldehyde, DIEA, NaCNBH₃, MeOH; (j) Cs₂CO₃, DMF or KF on alumina, 18-crown-6, CH₃CN.

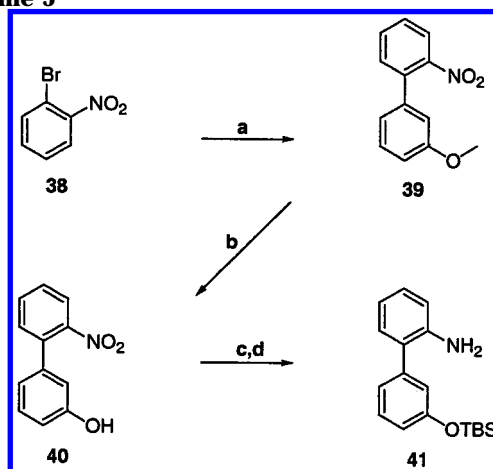
Scheme 4^a

^a Reagents: (a) NBS, AIBN, CCl₄; (b) AgNO₃, EtOH, H₂O; (c) MeMgBr, THF; (d) TBSCl, DMAP, Et₃N, CH₂Cl₂; (e) Tf₂O, DIEA, CH₂Cl₂; (f) TBAF, THF; (g) SO₃-pyridine complex, Et₃N, DMSO.

tended catalytic hydrogenation of **21** led to the deschloro intermediate **22** as separate diastereomers, which were then treated in the same way as **23** to provide analogues **26A** and **26B**.

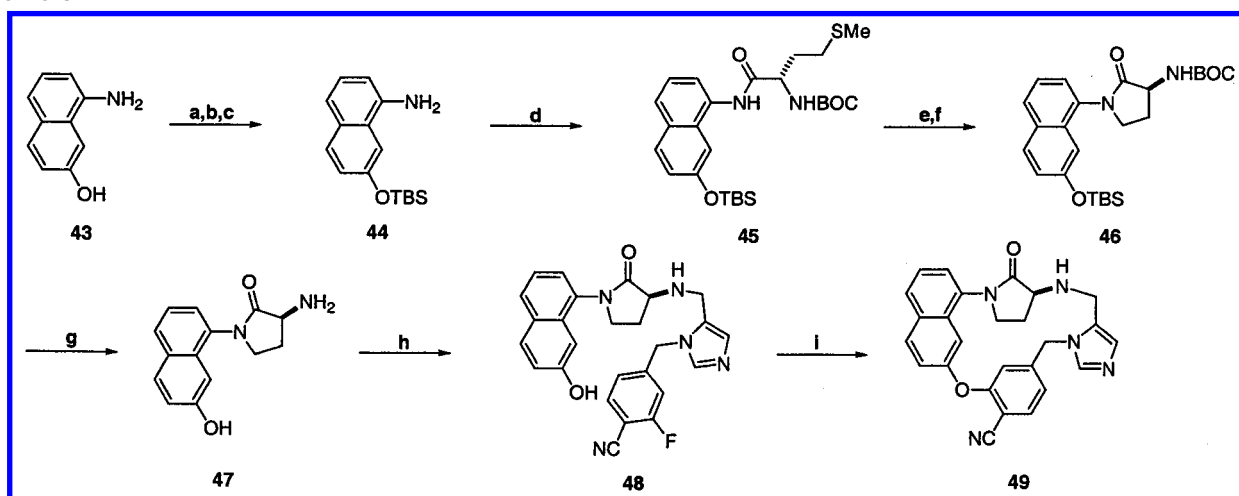
The preparation of aldehyde **35**, used to synthesize analogues **36A** and **36B**, is outlined in Scheme 4. Substituted toluene **28** was dibrominated with NBS, and treatment of **29** with AgNO₃ in EtOH afforded aldehyde **30**. Conversion of the aldehyde to benzyl alcohol **31** was accomplished by treatment with MeMgBr in THF. Alcohol **32** was protected with TBSCl, and the resulting silyl ether was reacted with the triflate of alcohol **31** to provide compound **34**. Deprotection of **34** and oxidation of the resulting alcohol led to the targeted aldehyde **35**. This aldehyde was reductively aminated with amine **9** and, by the same synthetic operations previously described, supplied **36A** and **36B**.

Bromo-2-nitrobenzene and (3-methoxyphenyl)boronic acid were reacted under Suzuki conditions to form the biphenyl template **39**, as shown in Scheme 5. Removal of the methyl group with BBr₃ in CH₂Cl₂ provided phenol **40**, which was protected as the *tert*-butyldimethylsilyl ether. Hydrogenation of the nitro group provided aniline **41**, which was elaborated in analogy with **44** (Scheme 6) to furnish **42**.

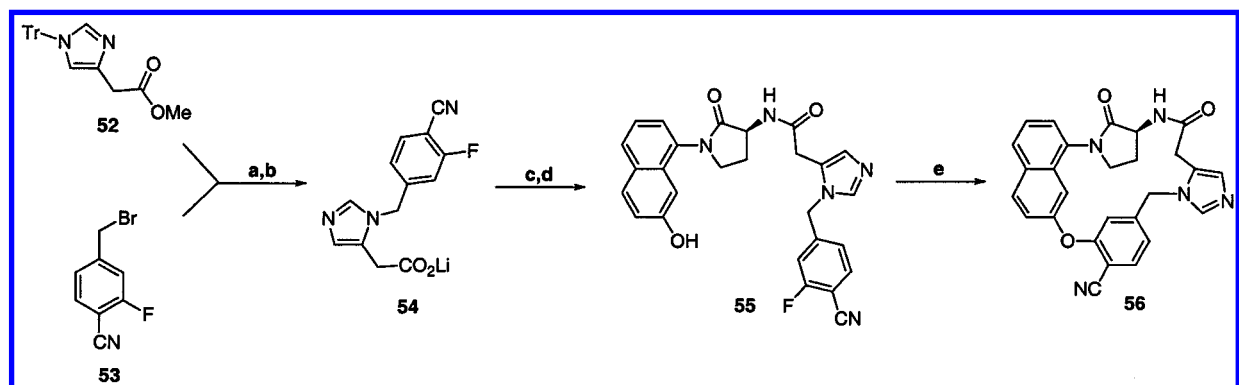
Scheme 5^a

^a Reagents: (a) (3-methoxyphenyl)boronic acid, (Ph₃P)₄Pd, K₂CO₃, DME; (b) BBr₃, CH₂Cl₂; (c) TBSCl, imidazole, DMF; (d) H₂, Pd/C, EtOH, EtOAc.

Incorporation of a naphthyl template provided rigid macrocycles such as **49**, as detailed in Scheme 6. Protection of the amino and phenolic functionalities of commercially available **43**, as the carbamate and TBS ether, respectively, followed by selective removal of the

Scheme 6^a

^a Reagents: (a) di-*tert*-butyl dicarbonate, DMF; (b) *tert*-butyldimethylsilyl chloride, imidazole, DMF; (c) HCl, EtOAc; (d) (*S*)-BOC-methionine, PyBOP, DIEA, CH₂Cl₂; (e) MeI; (f) Li(Me₃Si)₂N, THF; (g) HCl, EtOAc; (h) 1-(4-cyano-3-fluorobenzyl)-5-imidazolecarboxaldehyde, DIEA, NaCNBH₃, MeOH; (i) Cs₂CO₃, DMF.

Scheme 7^a

^a Reagents: (a) (i) CH₃CN; (ii) MeOH; (b) LiOH, THF, H₂O; (c) **47**, HOBT, EDC, DIEA, DMF; (d) TBAF, THF; (e) Cs₂CO₃, DMF.

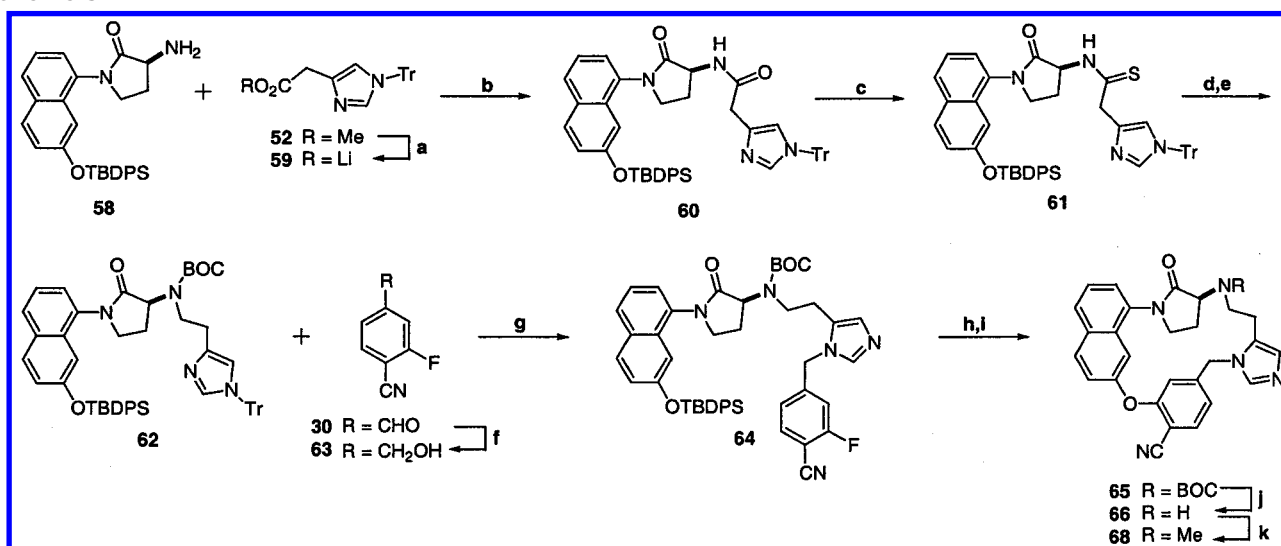
BOC group gave naphthylamine **44**. This aniline was converted to the pyrrolidinone **46** by the route previously outlined, and both protecting groups were removed under acidic conditions to afford **47**, which was then elaborated to give macrocycle **49**.

Analogues with two-carbon linkers between the amino group of the pyrrolidinone and the imidazole are depicted in Schemes 7 and 8. Production of the key intermediate **54** in Scheme 7 was achieved by reacting ester **52**⁸ and benzyl bromide **53**⁷ in CH₃CN, followed by methanolysis of the resulting imidazolium salt. Saponification afforded **54**, which was coupled to amine **47** by use of EDC and HOBT. The resulting amide was deprotected to give **55**, which was treated with Cs₂CO₃ in DMF to afford **56**.

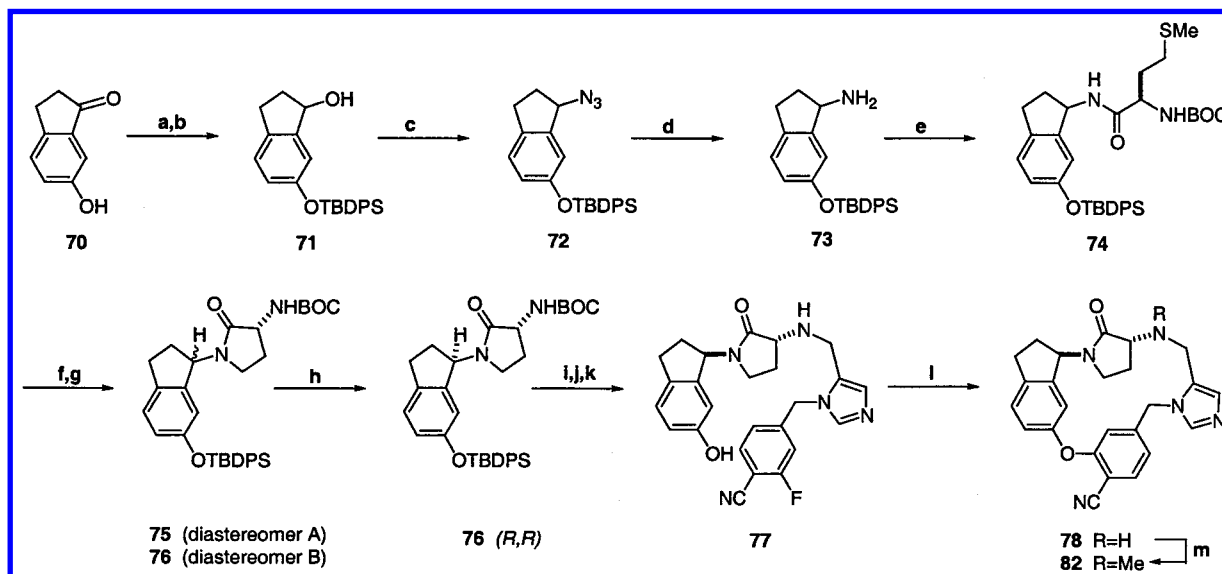
Synthesis of the homologated analogue of **49** was carried out via a different synthetic route, as illustrated in Scheme 8. Amine **58** was acylated with **59** to give **60**, which was subjected to Lawesson's reagent in THF. Thioamide **61** was reduced with NiCl₂ and NaBH₄ in EtOH, and the amine produced was protected as the *tert*-butyl carbamate to provide **62**. The triflate of alcohol **63** was prepared and reacted with **62** to give **64**, which was readily converted to the corresponding phenol and then macrocyclized to furnish **65**. Standard deprotection gave the desired macrocycle **66**, and reductive alkylation of **66** with formaldehyde produced the tertiary amine **68**.

An example of the preparation of indanyl analogues is illustrated in Scheme 9. Indanone **70** was prepared as the *tert*-butyldiphenylsilyl ether, which was found to offer a significant advantage over *tert*-butyldimethylsilyl ether due to its reduced lability. Reduction gave **71**, and subjection of **71** to the previously described chemical operations provided a mixture of diastereomers **75** and **76**, which were easily separated by silica gel chromatography. The absolute configuration of these diastereomers was determined by reduction of the indanone with (*R*)-methyl oxazaborolidine and BH₃SMe₂ in CH₂Cl₂ to afford (*S*)-**71**.⁹ Treatment of (*S*)-**71** with DPPA afforded the azide (*R*)-**72** with clean inversion, and this was subjected to the procedures in Scheme 9 to provide a single diastereomer, **76**, which was therefore established as the *R,R* isomer. Indane **76** was taken forward to give the macrocyclic product, **78**, as shown. Finally, analogue **78** was methylated to give **82**. The other indanyl diastereomeric macrocycles were synthesized analogously, as were the tetralin analogues (**83** and **84**) and chromane derivatives (**85** and **86**).

To investigate the conformations of compounds in solution, they were studied by NMR spectroscopy in CD₃OD solution. Distance constraints were extracted from nuclear or rotating Overhauser effect spectroscopy (NOESY or ROESY spectra) by using the magnitude of the NOE between either a geminal methylene pair or *o*-aromatic protons as fixed internal reference distances

Scheme 8^a

^a Reagents: (a) LiOH, THF, H_2O ; (b) HOBT, EDC, DIEA, DMF; (c) Lawesson's reagent, THF; (d) NiCl_2 , NaBH_4 , EtOH; (e) di-*tert*-butyl dicarbonate, DMF; (f) NaBH_4 , MeOH; (g) (i) TF_2O , DIEA, CH_2Cl_2 , (ii) MeOH; (h) TBAF, THF; (i) Cs_2CO_3 , DMF; (j) HCl, EtOAc; (k) formaldehyde, DIEA, HOAc, NaCNBH_3 , MeOH.

Scheme 9^a

^a Reagents: (a) *tert*-butyldiphenylsilyl chloride, imidazole, DMF; (b) NaBH_4 , MeOH; (c) DPPA, DBU, toluene; (d) LiAlH_4 , THF; (e) (*R*)-BOC-methionine, PyBOP, DIEA, CH_2Cl_2 ; (f) MeI; (g) $\text{Li}(\text{Me}_3\text{Si})_2\text{N}$, THF; (h) silica gel chromatography; (i) HCl, EtOAc; (j) 1-(4-cyano-3-fluorobenzyl)-5-imidazolecarboxaldehyde, DIEA, NaCNBH_3 , MeOH; (k) TBAF, THF; (l) Cs_2CO_3 , DMF; (m) formaldehyde, HOAc, NaCNBH_3 , MeOH.

of 1.8 or 2.5 Å, respectively. Conformations that satisfied the distance constraint data were generated with the distance geometry algorithm JG¹⁰ and subsequently energy-minimized by the MMFF force field with MacroModel¹¹ to provide low-energy solution structures.

Biological Methods

Standard assays for inhibition of FTase and geranylgeranyltransferase type I (GGTase I), for binding of compounds to the hERG (human ether-a-go-go-related gene) channel, and for the cell-based radiotracer assay for FTase inhibition (CRAFTI) were performed as previously described.⁶

Functional inhibition of FTase was assessed in PSN-1 cells by quantitation of the extent of processing of the FTase substrate HDJ by standard Western blotting

protocols. PSN-1 human pancreatic tumor cells were incubated in the presence of the desired concentration of test compound for 7 h at 37 °C, and then lysed in RIPA buffer [40 mM Tris-HCl, pH 7.5, 150 mM NaCl, 0.1% sodium dodecyl sulfate (SDS), 0.5% sodium deoxycholate, 1% Triton X-100, and 0.1 mM ethylenediamine-tetraacetic acid (EDTA), plus protease inhibitors]. Lysates were subjected to SDS-polyacrylamide gel electrophoresis (PAGE) on 8% precast Novex Tris-glycine gels (Invitrogen, Carlsbad, CA) and then immunoblotted with antibodies specific for HDJ2 (Lab Vision Inc., Fremont, CA). Blots were developed with alkaline phosphatase-conjugated anti-IgG (Cappel Laboratories, West Chester, PA), followed by detection with ECF fluorescent alkaline phosphatase substrate (Amersham Pharmacia Biotech, Piscataway, NJ). Blots were scanned

on a Storm 840 imager (Amersham Pharmacia Biotech). Unprenylated and prenylated proteins were distinguished by virtue of their different electrophoretic mobilities. The percentage of unprenylated protein was determined by peak integration with Imagequant software (Amersham Pharmacia Biotech). EC₅₀ values were derived from dose-response curves with a four-parameter curve-fitting equation by use of SigmaPlot software (SPSS Inc., Richmond, CA). The assay was run independently in the presence and absence of 50% human serum to evaluate the effects of protein binding on the test compound.

Inhibition of human or dog CYP3A was evaluated with pooled liver microsomes and testosterone substrate. Testosterone (75 μ M) was incubated with liver microsomes (0.25 mg of protein/mL) for 10 min in the presence of a reduced nicotinamide adenine dinucleotide phosphate (NADPH) generating system with and without test compound (0.05–100 μ M). The 6 β -hydroxytestosterone formed was quantitated by liquid chromatography and mass spectrometry (LC-MS/MS) by use of the transitions m/z 305 \rightarrow 269 (6 β -hydroxytestosterone) and m/z 361 \rightarrow 163 (cortisone, internal standard). The IC₅₀ value was calculated by comparing the amount of 6 β -hydroxytestosterone formed in the presence of test compound to the corresponding control sample.

Pharmacokinetic studies in dogs were performed according to standard protocols. The compound was dosed to two dogs either intravenously (in dimethyl sulfoxide, DMSO) or orally (in 0.5% methocellulose suspension) and the resulting plasma levels were quantitated by LCMS. Some compounds were dosed intravenously in combination with five other compounds as described in Table 5. Class III electrophysiologic activity was assessed in anesthetized dogs with the compound of interest being administered by intravenous infusion in an escalating dose protocol. Plasma levels of compound and electrocardiogram data were determined before and during the infusions, and the effects on the QT_c interval were correlated with drug concentrations in plasma to yield an EC₁₀ value, the concentration of compound which prolonged the QT_c interval by 10%.

X-ray crystal structures of the ternary complexes of human FTase with inhibitors **49** and **66** were determined as follows. Farnesyltransferase was concentrated to 10 mg/mL and combined with farnesyl diphosphate (FPP) and inhibitor dissolved in 25 mM DMSO in a 1:3:1.5 molar ratio. Diffraction-quality crystals were grown by the hanging drop vapor diffusion method from a mother liquor of 200–400 mM ammonium acetate and 12–14% poly(ethylene glycol) (PEG) 8K, pH 5.3–5.5, at 17 °C. Diffraction data were collected at cryogenic temperature on an *R*-axis IV image plate (Molecular Structure Corp.) mounted on a Rigaku RU-200 rotating anode X-ray source with double mirror optics. Data were reduced with DENZO and SCALEPACK.¹² The space group of the crystals was determined to be *P*6₁ with cell dimensions $a = b = 178.1$ Å and $c = 64.5$ Å. Phases were obtained by molecular replacement with farnesyltransferase, Protein Data Bank accession number 1JCQ.¹³ Model building proceeded using the program O¹⁴ and the coordinates were refined using the program CNS.¹⁵ Diffraction data and final refinement statistics are summarized in the Supporting Information. Coordi-

ates have been deposited in the Protein Data Bank with accession numbers 1LD8 and 1LD7.

Results and Discussion

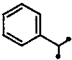
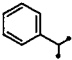
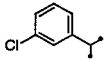
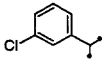
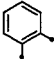
Potency and Selectivity. As part of an initial exploration of macrocyclic 3-aminopyrrolidinone FTIs, we synthesized the 1-benzylpyrrolidinone enantiomers **11** and **12** (see Table 1). We were gratified to find that the *R* enantiomer (**11**) was essentially equivalent to the highly potent FTI **1** in the cell-based assay for binding to FTase (CRAFTI IC₅₀ = 0.66 nM, see Table 1). The macrocycle **11** also displayed a very favorable ratio of intrinsic potency against the enzyme (FTase IC₅₀ = 3.5 nM) to cell-based activity, as had been seen previously for **1** and other 3-aminopyrrolidinone FTIs.⁶ It was also equipotent with **1** in a functional assay for cellular inhibition of FTase, in which inhibition of HDJ2 processing was assessed in the absence of added human serum (see Table 4). In this functional assay, the macrocycle **11** was shifted only about 2-fold by the addition of 50% human serum (HDJ EC₅₀ = 13 nM), whereas the noncyclic analogue **1** shifted more than 10-fold (HDJ EC₅₀ = 62 nM). This functional measure of the effects of added serum protein provides an estimate of the consequences of in vivo protein binding and the data indicated that macrocyclization of these FTIs significantly reduced the impact of human protein binding.

In contrast to linear 3-aminopyrrolidinone FTIs such as **1**, in which a stereochemical preference for the (*S*)-aminopyrrolidinone was observed in terms of inhibition of FTase,⁶ the related macrocycles exhibited a preference for the *R* stereochemistry. While the origins of this preference are uncertain, it was generally observed for such 1-benzylpyrrolidinone macrocyclic analogues (data not shown) and only the 3-(*R*)-pyrrolidinones are shown for the other structures in Table 1. All the compounds in Table 1 exhibited good selectivity for FTase over GGTase I.

One of the major concerns with **1** and other FTIs was prolongation of the QT_c interval in vivo (vide supra). This activity may have been due, in part, to the affinity of **1** for the hERG potassium channel [hERG IP (inflection point) = 440 nM], since blockade of this channel can predispose individuals to arrhythmias.⁶ We were therefore encouraged to find that **11** exhibited reduced activity against the hERG channel (hERG IP = 4700 nM). Moreover, this correlated with an in vivo assay for QT_c prolongation: in anesthetized dogs, intravenous (iv) infusion of **11** did not cause significant prolongation of the QT_c interval at plasma levels of 12 μ M (QT_c EC₁₀ > 12 μ M), a notable improvement over compound **1** (vide supra). Thus, the macrocyclic modification of 3-aminopyrrolidinone FTIs afforded a highly potent inhibitor with an improved profile in terms of class III activity and this encouraged us to explore further analogues of **11**.

Previously, we had discovered that the chloro substituent in **1** contributed approximately an order of magnitude to its potency against FTase,⁶ and this indicated that the benzyl substituent on the pyrrolidinone ring participated in important hydrophobic interactions with the enzyme. We reasoned that it should be possible to exploit the same binding pocket in the context of a macrocycle like **11**. Assuming that the

Table 1. Macrocyclic 3-Aminopyrrolidinone Inhibitors of FTase: Substituted Benzylpyrrolidinones

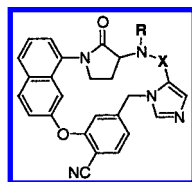
Compound	W	X	Y	Z	stereo ^a	FTase	GGTase	CRAFTI	hERG
						IC ₅₀ (nM) ^b	IC ₅₀ (nM) ^b	IC ₅₀ (nM) ^b	IP (nM) ^b
11	H	H	H	CH ₂	R	3.5 ± 1.5 (3)	> 20,000 (2)	0.66 (2)	4,700 (1)
12	H	H	H	CH ₂	S	54 (2)	> 20,000 (2)	13 (2)	11,000 (2)
16	H	Cl	H	CH ₂	R	23 (2)	> 20,000 (2)	6.4 (2)	220 (2)
26A	H	H	H		R, A ^c	58 (2)	1,600 (1)	230 (1)	320 (1)
26B	H	H	H		R, B ^d	10 (1)	5,800 (2)	34 (1)	2,900 (1)
27A	H	H	H		R, A ^c	25 (2)	820 (1)	210 (1)	82 (1)
27B	H	H	H		R, B ^d	2.5 (2)	7,000 (2)	200 (1)	530 (2)
36A	CH ₃	H	H	CH ₂	R, A ^c	170 (2)	> 20,000 (3)	74 ± 61 (4)	20,000 (2)
36B	CH ₃	H	H	CH ₂	R, B ^d	1.9 (2)	> 20,000 (3)	0.87 (2)	8,400 (2)
37	H	H	Br	CH ₂	R	1.4 (2)	9,200 (1)	0.19 (2)	4,600 (2)
42	H	H	H		R	1.3 (2)	810 (1)	0.032 ± 0.005 (3)	2,800 (2)

^a Stereochemistry at C-3 of pyrrolidinone. ^b Number of replicates used to determine IC₅₀ values shown in parentheses. ^c Diastereomer A. ^d Diastereomer B.

cyanophenyl, imidazole, and pyrrolidine rings in **1** and **11** could be approximately superimposed in the active site of FTase, the possible binding sites of the potency-enhancing chlorophenyl ring would describe a cone around an axis defined by the bond from the pyrrolidine nitrogen atom to the benzylic carbon. Solution NMR spectroscopy studies (vide infra) showed that compound **11** possessed significant flexibility, with the 1-benzyl substituent on the pyrrolidinone being highly mobile (see Figure 3A). Thus, we reasoned that we could explore a large fraction of the putative chlorophenyl-binding sites via simple substitution of this benzyl functionality. This led to macrocyclic analogues in which the chlorophenyl moiety is either coincident with the benzyl group's aromatic ring or rotated around the C–N bond axis by 120° increments (see compounds **16**, **27A**, and **27B** in Table 1). The diastereomeric deschloro analogues **26A** and **26B** were also synthesized as controls. As the data in Table 1 show, the most potent FTI in this series (**27B**) was essentially equipotent with the unsubstituted macrocycle **11**, demonstrating that, at best, the chlorophenyl moiety was tolerated but not beneficial. Moreover, the addition of this group in **27B** caused a profound loss in terms of cell-based inhibition

of FTase (CRAFTI IC₅₀ = 200 nM), perhaps due to impaired cell penetration properties associated with increased lipophilicity. The control compounds **26A** and **26B** indicated that, for both diastereomers, the addition of the chloro substituent enhanced intrinsic potency against FTase about 2–4-fold but offered no benefit in terms of cell activity. The observation that *m*-chloro substitution of **11** to give **16** led to a significant loss in inhibitory activity against FTase, both intrinsically and in cells, suggested that there was limited space in the enzyme's active site around this phenyl group. If this phenyl ring was indeed occupying a well-defined binding pocket, it seemed likely that it may be positioned in the same region occupied by the chlorophenyl ring in compound **1** and that the macrocycle **11** was already taking advantage of binding interactions similar to those of compound **1**.

Since metabolism of the benzylic sites in **11** was a potential concern, a number of modifications at these sites were explored. We initially synthesized the diastereomers **36A** and **36B** in which the 4-cyanobenzyl position was substituted with a methyl group (see Table 1). The importance of this region to productive interaction with FTase is illustrated by the IC₅₀ values of these

Table 2. Macrocyclic 3-Aminopyrrolidinone Inhibitors of FTase: Naphthylpyrrolidinones

compound	X	R	stereo ^a	FTase IC ₅₀ ^b (nM)	GGTase IC ₅₀ ^b (nM)	CRAFTI IC ₅₀ ^b (nM)	hERG IP ^b (nM)
49	CH ₂	H	S	3.5 ± 1.8 (4)	650 ± 150 (4)	3.8 ± 0.65 (3)	10 500 ± 600 (3)
50	CH ₂	H	R	1.6 (2)	3900 ± 1500 (3)	4.4 ± 2.5 (3)	8300 (1)
51	CH ₂	CH ₃	S	4.9 (2)	2200 (2)	39 (2)	4400 (2)
56	COCH ₂	H	S	2.1 ± 0.13 (3)	94 (2)	6.8 (1)	10 000 (2)
57	COCH ₂	H	R	2.3 (2)	150 (1)	13 (1)	9900 (2)
66	CH ₂ CH ₂	H	S	1.1 (2)	5.5 (2)	0.32 (4)	8100 (2)
67	CH ₂ CH ₂	H	R	1.2 (2)	35 ± 23 (3)	0.44 ± 0.17 (3)	210 ± 110 (3)
68	CH ₂ CH ₂	CH ₃	S	1.5 (2)	32 (2)	0.21 (2)	4900 ± 3900 (3)
69	CH ₂ CH ₂	CH ₃	R	1.2 (2)	39 (2)	0.57 (2)	180 (2)

^a Stereochemistry at C-3 of pyrrolidinone. ^b Number of replicates used to determine IC₅₀ values shown in parentheses.

diastereomers, which differ by almost 2 orders of magnitude. The more potent isomer, **36B**, exhibited similar intrinsic potency to the parent structure **11** and this translated into the cell-based assay (CRAFTI IC₅₀ = 0.87 nM).

Modification of the other benzyl group in **11** produced improved inhibitors of FTase. The bromo analogue **37** (Table 1) exhibited about 3-fold enhanced potency in both intrinsic and cell-based assays of FTase inhibition. Additionally, the potency of **37** in the cell-based functional assay was not altered by the presence of human serum (see Table 4). Replacement of the methylene unit in **11** with a phenylene moiety gave **42** (Table 1). While this change had a minimal effect on intrinsic potency against FTase in the standard assay, it increased the compound's cell potency by 20-fold to afford the first compound with an IC₅₀ value in this assay below 100 pM (CRAFTI IC₅₀ = 0.032 nM). Since a 60-fold difference between cell-based and intrinsic IC₅₀ values against FTase seemed unlikely, and since the standard enzyme assay was run with [FTase] = 1 nM, making it unable to accurately quantitate compounds with IC₅₀ values below low nanomolar concentrations, compound **42** was evaluated in a similar assay with [FTase] = 10 pM. In this modified assay, **42** was found to have FTase IC₅₀ = 0.060 nM, which agreed well with the result from the CRAFTI assay. For comparison purposes, **11** was evaluated in this modified FTase assay and found to have FTase IC₅₀ = 2.0 nM, a value essentially identical to that determined with [FTase] = 1 nM. The biphenyl-containing **42** was also highly potent in the cell-based HDJ2 processing assay (HDJ EC₅₀ = 0.67 nM) and the level of inhibition was unaffected by addition of human serum (see Table 4). Clearly, the biphenyl unit in **42** was taking advantage of some important interactions with FTase, highlighting the critical nature of this region of the macrocycle. Both **37** and **42** maintained good selectivity between FTase and the hERG potassium channel.

As previously described, 1-naphthylpiperazine-based macrocycles such as **3** had been found to be potent FTIs.⁷ Both enantiomers of the 3-aminopyrrolidinone analogue of this piperazine were synthesized, but in these cases the impressive subnanomolar potency of **3** was not realized (see Table 2). Additionally, the favor-

able ratio of cell-based to intrinsic potency that had been observed for many related 3-aminopyrrolidinones, such as **11** (FTase:CRAFTI = 5), was not seen for **49** (FTase:CRAFTI = 1) or its enantiomer (**50**), perhaps because of the more lipophilic nature of naphthyl compared with benzyl. Indeed, **49** and **50** were essentially equipotent in the CRAFTI assay, reflecting their very similar intrinsic potency against FTase. This behavior contrasted with that of the 1-benzylpyrrolidinone analogues in Table 1 but seemed to be quite general for the 1-naphthylpyrrolidinone macrocycles, and it suggested that the enzyme makes no key interactions with the aminopyrrolidinone moieties of these analogues. The attenuated cell potency of **49** also translated into the functional assay in PSN-1 cells (Table 4), in which it was 10-fold less potent than **11** both in the presence and in the absence of human serum. Although FTase did not discriminate between enantiomers **49** and **50**, the related enzyme GGTase I did show a 6-fold preference for the *S* isomer in terms of IC₅₀ value (see Table 2). Importantly, the interaction with the hERG channel appeared to be minimal for **49**, and this was consistent with the observation in dogs that iv infusion of **49** did not cause 10% prolongation of the QT_c interval at plasma levels of 7 μM (QT_c EC₁₀ > 7 μM).

One difference between the 3-aminopyrrolidinone and piperazinone backbones is that the pyrrolidinone contains a secondary amine. To investigate the role of this functionality, **49** was converted to the corresponding tertiary amine **51**, and it was found that this modification had only modest effects on the intrinsic potency of the molecule (see Table 2). In contrast, the tertiary amine was about 10-fold less potent in cells (CRAFTI IC₅₀ = 39 nM) as compared with **49**, consistent with the observation that tertiary amine analogues of **1** had reduced potency in cells.⁶ The origin of the attenuated cell potency is not known, but it is possible that the secondary amino functionality simply reduces the molecule's overall lipophilicity and that this promotes cell penetration. However, previous studies⁶ indicate that 3-aminopyrrolidinones such as **1** are poor substrates for the P-glycoprotein pump, which can be a major factor in reducing efficacy in cells,¹⁶ and the secondary amino group may be partly responsible for this behavior.

The enantiomers **49** and **50** were isomers of FTI **3** in which the piperazinone ring was replaced by an aminopyrrolidinone moiety, and this change caused a potency loss of more than an order of magnitude. Several lines of evidence suggested that this modified portion of the macrocycle did not make critical contacts with FTase, and later X-ray crystallographic studies confirmed this (vide infra). Thus, the role of the piperazinone/aminopyrrolidinone moiety was to correctly orient the [4-cyano-3-(naphthyl)benzyl]imidazole pharmacophore and, apparently, the aminopyrrolidinone in **49** and **50** did not allow these key pharmacophoric elements to bind optimally to the active site. We reasoned that ring expansion of the macrocycles **49** and **50** might permit improved binding to FTase since the expanded molecules should be less rigid.

The first ring-expanded compounds, the acetamide-linked analogues **56** and **57** (17-member macrocycles), were similar as FTIs to the corresponding methylene-linked enantiomers **49** and **50** (16-member macrocycles) but showed increased activity against GGTase I (Table 2). Reasoning that the flexibility imparted by the increased macrocyclic ring size may have been countered by the inherent rigidity of the additional amide bond, we synthesized the ethylene-linked analogues **66** and **67**. As expected, removal of the amide carbonyl from **56** and **57** led to improvements in the potency against FTase. Thus, homologation of the methylene linker in **49** to ethylene in **66** increased potency in CRAFTI by more than 10-fold (for **66**, CRAFTI IC_{50} = 0.32 nM). In the functional HDJ2 processing assay, **66** was found to be improved by an order of magnitude compared to **49**, and this nanomolar potency was not shifted significantly by 50% human serum (see Table 4). The high levels of cell potency appeared to be due to an increase in intrinsic potency, consistent with the notion of a more flexible inhibitor than **49** having higher affinity for the enzyme. For compound **66**, for example, determination of FTase inhibition at 10 pM enzyme concentration revealed that its FTase IC_{50} = 0.19 nM. Both **66** and **67** were more than 100-fold improved as inhibitors of GGTase I, as compared to the nonhomologated enantiomers, **49** and **50** (see Table 2), although the ring-expanded compounds were still quite selective for FTase over GGTase I.

Interestingly, while the homologation to provide compounds such as **66** led to a significant improvement in affinity for FTase and GGTase I for both enantiomers, binding to the hERG channel was not affected for the *S* enantiomers (compounds **66** and **68**) but was significantly enhanced for the *R* enantiomers (compounds **67** and **69**). Thus, ring expansion of **49** to give **66** had little effect on the hERG IP, but homologation of **50** to afford **67** led to a 40-fold increase in affinity for the ion channel (Table 2). Importantly, evaluation of the *S* enantiomer **66** in dogs indicated that the compound had an EC_{10} value of $>8 \mu\text{M}$ for prolongation of the QT_c interval, which was consistent with its weak binding to the hERG channel and afforded a large window between significant effects on QT_c and plasma levels that would presumably inhibit FTase in vivo.

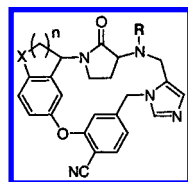
The *N*-methylated analogues **68** and **69** were prepared in an attempt to modestly rigidify aminopyrrolidinones **66** and **67** without significantly reducing affin-

ity for FTase. These analogues exhibited broadly similar properties to their desmethyl counterparts in terms of inhibitory activity (Table 2). Compound **68**, which had similar potency in the CRAFTI assay to **67**, was also found to have similar potency in the HDJ processing assay (HDJ EC_{50} = 6.9 nM, see Table 4). These observations contrasted with the case of structure **51**, in which the tertiary amine functionality apparently led to a reduction in relative cell-based potency (vide supra).

Macrocyclic ring expansion of **49**, leading to compound **66**, improved inhibitory potency against FTase more than 10-fold, presumably because the additional degrees of freedom in **66** permitted it to adopt a more optimal conformation in the enzyme's active site than **49**. An alternative strategy was to investigate analogues of **49** that would be similarly rigid but that would present a more optimal arrangement of the key [4-cyano-3-(aryl-oxy)benzyl]imidazole pharmacophore to the enzyme. Reasoning that the kink introduced into the backbone of **49** by the 3-aminopyrrolidinone moiety may partly explain its attenuated affinity for FTase relative to piperazinone-based FTIs such as **3**, we sought to introduce a compensating adjustment of the naphthyl ring system and targeted indanyl replacements. In these structures, the sp^2 carbon at the 1-position of the naphthyl ring is replaced by a sp^3 carbon, effectively shifting the aryl ring in the indane out of the plane occupied by the naphthyl system. All four diastereomers of this system were synthesized, and the results are detailed in Table 3 (compounds **78**–**81**).

The isomers exhibited markedly different potencies against FTase, with the *R,R* diastereomer (**78**) having an IC_{50} value < 1 nM. Redetermination of this IC_{50} with reduced enzyme concentration ($[FTase] = 10 \text{ pM}$) indicated that a more accurate value was 0.15 nM. Therefore, inversion of the indanyl stereocenter cost over 4 orders of magnitude in terms of intrinsic potency against FTase (for **79**, FTase IC_{50} = 1800 nM). These data indicate that the orientation of the aryl ring in the indane is critical for binding to FTase, consistent with other structure–activity relationships (SAR) and the X-ray crystal structures of enzyme–inhibitor complexes (vide infra). Changing the pyrrolidinone C-3 position from *R* in **78** to *S* in **80** also caused a significant drop in affinity for FTase. The cell assay for binding to FTase ranked the compounds in the same order, with **78** being the most potent (CRAFTI IC_{50} = 0.22 nM, see Table 3). Moreover, **78** was found to be a highly potent inhibitor of HDJ2 processing in PSN-1 cells and was not shifted by addition of human serum (HDJ EC_{50} = 3 nM, Table 4).

Unfortunately, just as the four diastereomers had widely varying affinities for FTase, their interactions with the hERG channel were not uniformly weak and the potent FTI **78** had a relatively high affinity for this potassium channel (hERG IP = 80 nM). Evaluation of **78** in anesthetized dogs revealed that it had a QT_c EC_{10} = $2.4 \mu\text{M}$, which was not as severe as the ion channel data suggested but was nonetheless unacceptable. The correlation between hERG binding data and in vivo effects on the QT_c interval was not perfect for the macrocycles described here, as has been observed for other FTIs.⁶ This may be due to many factors, including in vivo interactions with other ion channels, differential

Table 3. Macrocytic 3-Aminopyrrolidinone Inhibitors of FTase: Bicyclic Naphthyl Replacements

compound	X	n	R	stereo ^a	FTase IC ₅₀ ^b (nM)	GGTase IC ₅₀ ^b (nM)	CRAFTI IC ₅₀ ^b (nM)	hERG IP ^b (nM)
78	CH ₂	1	H	R,R	<1 (2)	18 000 (2)	0.22 (2)	80 ± 22 (3)
79	CH ₂	1	H	R,S	1800 (2)	20 000 (1)		4300 (2)
80	CH ₂	1	H	S,R	3.6 (2)	>20 000 (1)	41 (1)	4700 (2)
81	CH ₂	1	H	S,S	44 (2)	4000 (2)	93 (1)	2700 (2)
82	CH ₂	1	CH ₃	R,R	1.4 (1)	>20 000 (1)	0.64 (2)	2600 (2)
83	CH ₂	2	H	R,R	<1 (2)	390 (2)	0.054 (2)	7000 (2)
84	CH ₂	2	H	S,R	1.5 (2)	2200 (2)	0.21 (1)	12 000 (2)
85	O	2	H	R,R	<1 (2)	1100 (2)	0.063 (2)	150 (2)
86	O	2	H	S,R	4.9 (2)	15 000 (2)	1.8 (2)	9100 (1)

^a Stereochemistry at C-3 of pyrrolidinone followed by stereochemistry at bicyclic benzylic carbon. ^b Number of replicates used to determine IC₅₀ values shown in parentheses.

Table 4. Cellular Inhibition of FTase by Macrocytic 3-Aminopyrrolidinones

compound	HDJ processing EC ₅₀ ^a (nM)	HDJ processing + HS EC ₅₀ ^b (nM)	compound	HDJ processing EC ₅₀ ^a (nM)	HDJ processing + HS EC ₅₀ ^b (nM)
1	4.7 (1)	62 (1)	67	5.5 (2)	6.0 (1)
11	6.1 ± 1.2 (3)	13 (2)	68	6.9 (1)	10 (1)
37	1.6 ± 0.11 (4)	1.0 ± 0.87 (4)	78	3.0 (1)	3.0 (1)
42	0.67 (1)	0.58 (1)	83	0.18 (2)	0.25 (2)
49	48 ± 23 (3)	130 ± 63 (3)	84	3.0 (2)	4.4 (2)
66	4.3 ± 2.1 (5)	7.5 (2)	85	0.12 (1)	0.38 (1)

^a EC₅₀ value for the inhibition of processing of HDJ2 in PSN-1 cells in a 7 h assay. Number of replicates used to determine EC₅₀ values shown in parentheses. ^b Identical to the HDJ processing assay but run in the presence of 50% human serum.

protein binding of compounds, or species differences between the human and canine potassium channels. In general, however, it was observed that the macrocyclic FTIs produced less *QT_c* prolongation in vivo than non-macrocyclic FTIs that had similar affinities for the hERG channel, and **78** seemed to conform to these observations. Interestingly, while N-methylation of **78** had only a minor effect on potency in the CRAFTI assay, it led to significantly reduced binding to the hERG component of the I_{Kr} channel, again illustrating the capricious nature of binding to this channel (hERG IP = 2600 nM for **82**, compared with 80 nM for **78**). Since subtle structural variations appeared to significantly reduce the affinity of **78** for the hERG channel, we targeted analogues in which the overall topology was slightly modified by expansion of the cyclopentenyl ring in the indane (compounds **83–86** in Table 3). Indeed, SAR at this ion channel continued to be subtle: the simple homologue **83** possessed significantly attenuated binding relative to **78**, but affinity for hERG was restored by replacement of the C-4 methylene with oxygen (see compound **85**, Table 3).

The diastereomers of these homologues exhibited an order of activity against FTase similar to the indanyl compounds, so only the most potent isomers are shown in each case. In each case, the *R,R* isomer was found to be the most potent intrinsic inhibitor of FTase and this translated into CRAFTI IC₅₀ values below 100 pM. For such potent analogues, data from the modified enzyme assay run with 10 pM enzyme concentration might underestimate the inhibitory activity, but in this assay, it was determined that FTase IC₅₀ = 20 pM for **83**. The extremely high levels of cell activity in CRAFTI translated into the functional HDJ2 processing assay to

afford EC₅₀ values of 0.25 nM (for **83**) and 0.38 nM (for **85**) in the presence of 50% human serum (see Table 4). As judged by this processing assay, **83** and **85** are the most potent cell-based inhibitors of FTase that have been described. Clearly, a significant advantage in terms of FTase inhibition results from expansion of the indanyl five-membered ring. From another viewpoint, saturation of two vinylic bonds in the naphthalene ring of **50** (Table 2) to give **83** (Table 3) enhanced potency against FTase by approximately 2 orders of magnitude. This is probably due to a combination of introduction of an sp³ center at C-1 of the naphthalene, allowing the macrocycle to adopt a preferred conformation in the active site while maintaining some rigidity, and favorable hydrophobic interactions with the cyclohexene ring. In terms of potency and selectivity, compound **83** represented a significant improvement over the linear 3-aminopyrrolidinone **1**. Not only did this macrocycle possess significantly attenuated affinity for the hERG potassium channel (hERG IP = 7000 nM for **83**, compared with 440 nM for **1**) but it was 250-fold more potent than **1** as an inhibitor of FTase in the functional assay in the presence of human serum (see Table 4). Such observations indicated that the therapeutic window between efficacious plasma levels and those that could cause prolongation of the *QT_c* interval had been greatly improved compared with compound **1**.

X-ray Crystallography. As part of an effort to elucidate the key interactions between these macrocyclic pyrrolidinones and FTase, compounds **49** and **66** were co-crystallized with farnesyl diphosphate (FPP) and FTase, and the structures were determined by X-ray crystallography. Figure 2 shows views of the ternary complex active site with either **49** (Figure 2A) or **66**

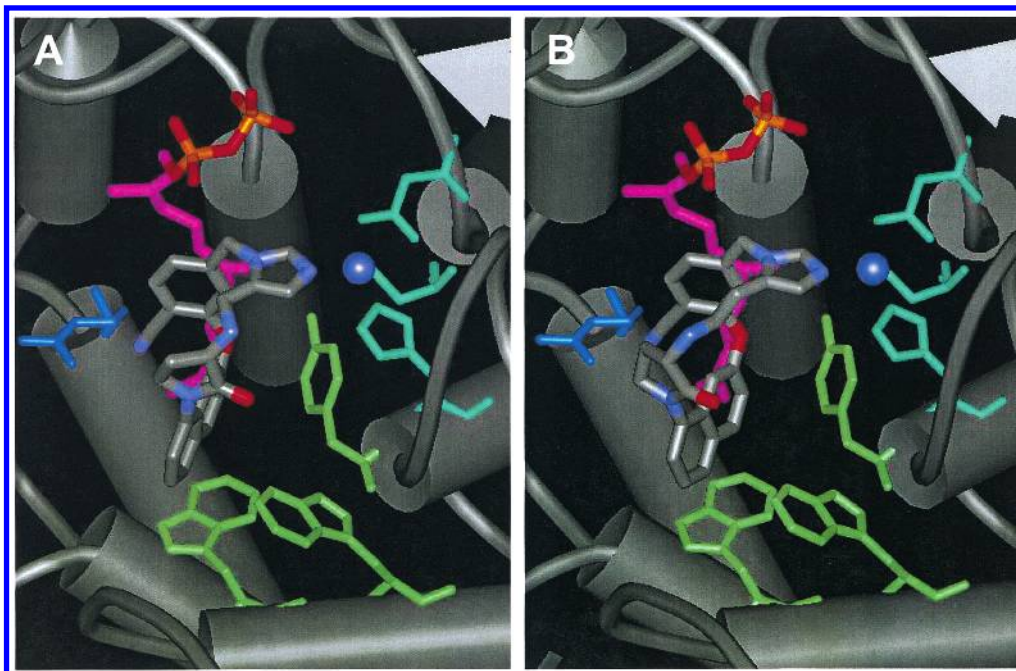


Figure 2. X-ray crystal structures of the FTase-FPP-FTI ternary complexes with compounds **49** (A) and **66** (B). The farnesyl group of FPP is colored magenta. The three zinc-ligating residues (Asp297, Cys299, His362) are shown in cyan, Arg 202 is shown in blue, and three aromatic side chains that define a hydrophobic pocket (Trp102, Trp106, Tyr361) are shown in green.

(Figure 2B), and it is readily seen that the structures are very similar. Indeed, the two structures of the FTase protein and its FPP substrate are essentially superimposable and a number of general points apply to the binding of the macrocycle in both complexes. As expected, the imidazole, which was introduced into this class of FTIs as a replacement for the thiol of the CaaX tetrapeptide substrate, is ligated to the catalytic zinc. The cyanobenzyl substituent, which provides a significant potency enhancement for many imidazole-containing FTIs,⁸ stacks against the FPP isoprenoid but it is not clear what specific role the critical cyano group plays. It may simply attenuate the electronics of the phenyl ring for optimal interaction with the prenyl group, but a more specific interaction with the protein could be considered. However, the closest amino acid side chain to the cyano group is that of Arg202 in the β -subunit (colored blue in Figure 2). It is positioned with its guanidine group about 3 Å from the nitrile nitrogen, but the relative geometry of the two groups does not appear consistent with a direct interaction. The naphthyl ring binds in a hydrophobic pocket defined by Trp102, Trp106, Trp303, and Tyr361 in the β -subunit. Other crystallographic studies have shown that this hydrophobic pocket interacts with the side chain of the second aliphatic residue in CaaX peptide substrates, such as Ile in CVIM.¹⁷ These observations are consistent with both the CaaX-competitive nature of these aminopyrrolidinone FTase inhibitors and the apparent importance of this aryl ring in their SAR. In both complexes, the pyrrolidinone ring is exposed to bulk solvent and the carbonyl oxygen is oriented toward solvent. Since the various pairs of enantiomers in Table 2 have similar potency against FTase, and since it is energetically unlikely that they all bind to the enzyme with the pyrrolidinone carbonyl oriented in the same direction, we conclude that the orientation of this functionality has little effect on binding to the enzyme.

Thus, the complexes of FTIs **49** and **66** with the enzyme are extremely similar and this prompts a simple question: can the improved potency of **66** compared to **49** be explained? One possible answer is that the compounds interact identically with the enzyme but that the bound conformation of **49** is more strained than that of **66**. In other words, is the bound conformation of **49** higher in energy than that of **66**, compared to their corresponding unbound energies? To address this, we generated random conformations of both molecules with JG¹⁰ and energy-minimized these conformers with MacroModel.¹¹ For each compound, the conformer that most closely resembled the enzyme-bound structure was compared to the lowest energy conformer. Thus, it was determined that the bound conformation of **49** was 6 kcal·mol⁻¹ higher than its lowest energy conformer whereas for **66**, the energy difference was 8 kcal·mol⁻¹. For this kind of analysis, these values are not significantly different, and in any case, this suggests that the bound conformation of **66** is slightly higher in energy than that of **49**. Another explanation is that the compounds do, in fact, interact differently with the enzyme, with **66** binding in a more optimal mode. Analysis of the crystal structures of the two ternary complexes revealed that when the protein backbones are superimposed, the (cyanobenzyl)imidazole moieties in **49** and **66** overlay exactly. The major difference in the structures is that the aminopyrrolidinone in **66** is rotated away from the zinc ion and the naphthyl ring is rotated concomitantly (see Figure 2). While SAR evidence indicates that the aminopyrrolidinone makes no significant interactions with the enzyme, the naphthyl ring is extremely important (vide supra). Compared to the **49** ternary complex, the naphthyl ring in enzyme-bound **66** is rotated further into the hydrophobic pocket (shown in green in Figure 2) and is positioned in a more perpendicular fashion with respect to the Trp102 indole ring. Studies of protein crystal structures and calcula-

Table 5. Dog Pharmacokinetic Data for Macrocytic 3-Aminopyrrolidinones

compound	iv dose ^a (mg·kg ⁻¹)	CL _p (mL· min ⁻¹ ·kg ⁻¹)	Vd _{ss} (L·kg ⁻¹)	iv t _{1/2} (h)	F ^b (%)
1	1	5.8	0.45	1.1	81 (3)
11	1	9.0	0.57	0.78	47 (2)
36B	0.5	12	0.69	0.78	
37	0.5 ^c	3.2	0.53	1.6	
42	0.5 ^c	8.0	0.61	0.88	
49	1	1.1	0.34	3.6	68 (1)
50	1	2.8	0.42	1.7	
51	0.5 ^c	0.26	0.21	10.1	
56	0.5 ^c	1.5	0.19	1.7	
66	1	3.9	0.57	2.0	92 (3)
68	0.5 ^c	1.4	0.25	1.9	
78	0.5 ^c	2.1	0.27	1.7	
80	0.5 ^c	1.3	0.50	4.2	
83	0.5 ^c	7.3	0.36	0.48	
85	1	5.5	0.34	0.90	

^a Dose of compound given to dogs intravenously, either as a single compound or in a combination dosing study. ^b Dose of compound used for oral PK study shown in parentheses. ^c Dosed iv in combination with five other compounds.

tions have indicated that the optimal angle between two aryl rings in an edge–face interaction is 90°, i.e., in a perpendicular orientation.^{18–20} The angle between the naphthyl and indole rings is 83° for the **66** complex and 103° for the **49** complex, suggesting that this interaction in the **66** complex may be more optimal. It seems possible that this small adjustment contributes to the 10–20-fold enhanced potency of **66** vs **49**. Interestingly, this change in the enzyme-bound orientation of the naphthyl ring from **49** to **66** is consistent with the SAR observed for the compounds in Table 3 (vide supra). Specifically, the effect of replacing the naphthyl ring with an *R*-indanyl ring is to shift the plane of the aryl ring in the same direction as it is shifted in **66** relative to **49**. This stereochemical preference for such an *R* stereocenter was seen for all the analogues in Table 3, reinforcing the idea that the rotation of the naphthyl ring seen in the crystal structure of the **66** complex (compared to the **49** complex) may be responsible for the enhanced potency of **66**.

Pharmacokinetics and Structural Rigidity. One of the main objectives of this work was to improve the plasma half-life of FTIs such as **1**, to minimize the ratio of drug concentration peak to trough following oral dosing. Evaluation of the pharmacokinetic behavior of the prototypical 3-aminopyrrolidinone macrocycle **11** (Table 1) in dogs revealed that it had an iv half-life of 0.78 h and oral bioavailability of 47% (see Table 5) and therefore offered no advantage over **1** in terms of pharmacokinetic profile.

Drug metabolism studies had shown that oxidative metabolism at the benzylic carbon of the (cyanobenzyl)-imidazole moiety was a perennial problem for FTIs containing this functionality. Incorporation of a methyl group at this benzylic site to give compound **36B** was undertaken in an attempt to reduce such metabolism. Disappointingly, the half-life of **36B** following iv dosing of dogs was identical to that of **11** and the plasma clearance was not improved (CL_p = 12 mL·min⁻¹·kg⁻¹), demonstrating that simple steric blockade of one of the putative metabolic sites had no beneficial effects in this case (see Table 5).

To gain insight into the conformational preferences of a macrocycle like **11**, the compound was studied by

NMR spectroscopy in CD₃OD solution. While sharp resonances were seen in the proton spectrum at 25 °C, many of the resonances displayed differential broadening upon cooling to temperatures below –20 °C. This result was characteristic of chemical exchange between multiple conformers and indicated that the spectrum at room temperature represented an “averaged” conformation. Nonetheless, a NOESY spectrum was acquired at 25 °C, the observed NOEs were used to derive distance constraints between protons, and these constraints were used to generate energy-minimized conformers. The experiment can provide information about the solution conformation of the free inhibitor, and representative results are illustrated in Figure 3. The results for analogue **11** revealed no single conformer that could satisfy all the NOE-generated distance constraints, again indicative of a flexible molecule. Conformers that satisfied the majority of the constraints could be generated but not ranked in terms of energy, since they did not all satisfy the same distance constraints. Thus, Figure 3A shows *all* 40 conformers generated and clearly illustrates the highly mobile nature of this macrocycle. (For comparison purposes, the 40 *lowest energy* structures are shown for the other compounds in Figure 3). The methylated macrocycle **36B** was studied in an analogous NOESY study and, in this case, conformers that satisfied all of the distance constraints were generated. The results are illustrated in Figure 3B and it was apparent that while methyl substitution at the benzylic position in **36B** had increased the molecule's rigidity compared with **11**, the ensemble of conformations was still indicative of moderate flexibility.

It was, of course, possible that the other benzylic site in **11** was also a major focus of oxidative metabolism, and a number of modifications of this site were studied. The bromo analogue of **11** (compound **37** in Table 1) possessed attenuated plasma clearance, which afforded a 2-fold improvement in t_{1/2} (see Table 5). Replacement of the benzylic group with a biphenyl moiety gave compound **42**, which, while highly potent as an FTI (vide supra), was also a very potent inhibitor of the cytochrome P₄₅₀ enzyme CYP3A4 (CYP3A4 IC₅₀ < 0.05 μM, Table 6). Additionally, compound **42** offered no significant improvement over **11** in terms of plasma clearance or half-life (see Table 5). Thus, removal of this benzylic methylene and replacement by a phenylene moiety did not improve pharmacokinetic properties, but installation of an *o*-bromo substituent did reduce clearance and increase half-life. Modifications in this region, therefore, had the potential to enhance such properties.

Another modification of the 1-benzyl substituent on the pyrrolidinone was conversion to a naphthyl ring, to give the enantiomers **49** and **50**. Evaluation of the pharmacokinetics of the *S* enantiomer (**49**) in dogs demonstrated that this modification had a significant impact (see Table 5). The compound substantially outperformed previous analogues such as **1** and **11**, with a half-life of 3.6 h and bioavailability of 68%. The improved half-life was due to a significantly reduced plasma clearance (CL_p = 1.1 mL·min⁻¹·kg⁻¹) and this demonstrated that the metabolic liabilities of the (cyanobenzyl)imidazole group could be overcome in the context of such a macrocycle. Importantly, inhibition of

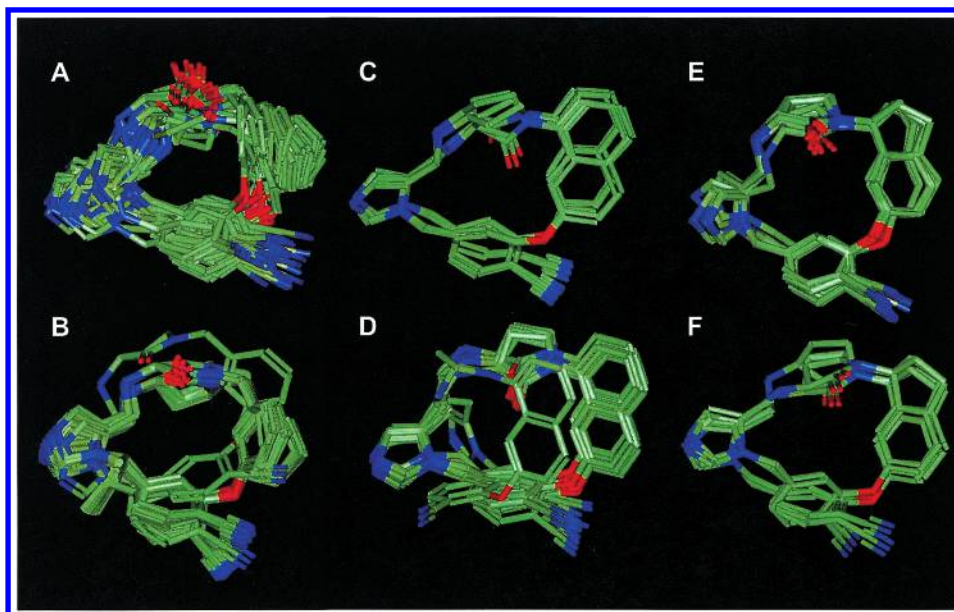


Figure 3. Solution structures determined by NMR spectroscopy in CD₃OD for compounds **11** (A), **36B** (B), **49** (C), **66** (D), **78** (E), and **80** (F). Distance constraints were extracted from a NOESY spectrum and calibrated relative to an NOE observed between two protons separated by a defined distance. Energy-minimized conformers that satisfied the NOE-derived distance constraints were generated, and the 40 lowest energy conformers are shown in each case. For structure **11**, no conformers satisfied all the NOE constraints and all 40 structures obtained are shown.

Table 6. Inhibition of CYP3A by Macrocycles

compound	human CYP3A4 IC ₅₀ (μM)	dog CYP3A IC ₅₀ (μM)
1	1.0	
11	8.9	
36B		6.1
37	6.1	
42	<0.05	
49	8.0	5.0
51	5.0	
56	8.1	
66	6.0	0.6
78	6.6	10.4
80	2.8	14.8

P₄₅₀ enzymes did not appear to be responsible for the observed low clearance. While CYP3A4 was the isozyme primarily responsible for microsomal metabolism of all the FTIs examined in this class, the CYP3A4 IC₅₀ value for **49** was essentially the same as that for more rapidly cleared compounds such as **11**, and there was no significant difference for **49** between human CYP3A4 and dog CYP3A (see Table 6).

The positive pharmacokinetic attributes of compound **49** caused us to focus our efforts on this structural class and, specifically, to attempt to address the reasons why **49** exhibited significantly lower clearance than the closely related macrocycle **11**. NMR spectroscopy studies on **49** showed essentially no line broadening upon cooling the sample from 25 to −50 °C, suggesting that the compound was extremely rigid, with the possibility that a single conformation existed in solution. A NOESY study conducted on **49** in CD₃OD at 25 °C resulted in a set of energy-minimized conformers that satisfied all the distance constraints. Figure 3C shows the 40 lowest-energy conformers derived from the NOESY data for compound **49**. The remarkable rigidity of this macrocycle was evident from the fact that all 40 conformers showed only minor conformational perturbations from one another. Moreover, an analogous experiment con-

ducted in CD₃OD at −50 °C gave results essentially identical to those shown in Figure 3C. It seemed possible that such structural rigidity could contribute to the low clearance of **49**, by reducing the molecule's ability to adopt conformations that permit facile oxidative metabolism at, for example, the benzylic carbon. Consideration of the rigidity of **49** could also explain why it was not more potent as an inhibitor of FTase, since it may prevent the molecule from presenting the [4-cyano-3-(aryloxy)benzyl]imidazole pharmacophore in an optimal arrangement (vide supra). The results for **11** and **36B** (Figure 3A,B), which are more rapidly cleared in vivo (Table 5), are consistent with the proposal that these more flexible analogues can present conformations to, for example, CYP3A that allow facile, rapid oxidation to take place.

Thus, rigidity may play a key role in attenuating the metabolic clearance of this series of macrocycles but it is clearly not the only important parameter. This is illustrated by the results for the enantiomer of **49**, which possessed a 2-fold shorter plasma half-life that was primarily due to increased clearance ($CL_p = 2.8 \text{ mL} \cdot \text{min}^{-1} \cdot \text{kg}^{-1}$). While **50** possessed the same rigidity as **49**, the metabolic clearance of this enantiomer may have been higher due to the asymmetric nature of the metabolizing enzymes. The complexity of the situation is further illustrated by the fact that **51** possessed an even lower plasma clearance than **49** ($CL_p = 0.26 \text{ mL} \cdot \text{min}^{-1} \cdot \text{kg}^{-1}$ for **51**; see Table 5), affording an impressive 10.1 h plasma half-life. It may be expected that the additional methyl group in **51** would further rigidify this portion of the molecule, promoting even greater resistance to metabolic enzymes. However, demethylation of such a tertiary amine is often a facile metabolic process. Moreover, differences in lipophilicity ($\log P = 2.27$ for **49** and 2.77 for **51**) or protein binding (dog protein binding = 94% for **49** and 99% for **51**) may also play a role in modulating metabolism. Despite these

complications, we believed that the low clearance of **49** was related, in part, to its rigidity and attempted to incorporate this concept into the design of other analogues.

As described previously, we anticipated that the potency of **49** as an FTI may be enhanced if the linker between the naphthyl ring and the imidazole were lengthened, allowing a greater degree of flexibility, and the results were generally in accord with this (see Table 2). The concern with this strategy was whether such increased flexibility would lead to higher rates of metabolism. Pharmacokinetic analysis of the initial ring-expanded macrocycle, **56**, revealed that the observed plasma clearance was similar to that observed with **49**, although the half-life was attenuated by a lower volume of distribution (see Table 5). However, this analogue was no more potent as an FTI than **49** (vide supra), and these results were consistent with the notion that the acetamide-linked **56** was not significantly more flexible than **49**.

Removal of the amide carbonyl in the acetamide linker of **56** provided **66**, and ¹H NMR spectroscopic analysis found that at temperatures above -35 °C chemical exchange broadening of resonances was evident. This result indicated that the compound existed as a mixture of conformations and precluded a detailed structural analysis at these temperatures. Below -35 °C, however, two distinct conformers were resolved and a ROESY experiment at -50 °C allowed distance constraints to be obtained for both conformers, which led to the energy-minimized structures shown in Figure 3D. These results indicated that **66** was intermediate between **11** and **49** in terms of rigidity, suggesting that the plasma clearance would be higher than that of **49**. The dog pharmacokinetic data for **66** were consistent with these expectations: $CL_p = 3.9 \text{ mL} \cdot \text{min}^{-1} \cdot \text{kg}^{-1}$; iv $t_{1/2} = 2.0 \text{ h}$; oral bioavailability = 92% (see Table 5). In analogy with the results for **49** and **51**, N-methylation of **66** was explored in an attempt to reduce in vivo clearance and this provided compound **68**. The pharmacokinetic data for **68** did reveal a reduction in clearance ($CL_p = 1.4 \text{ mL} \cdot \text{min}^{-1} \cdot \text{kg}^{-1}$) compared with **66** as expected, but the plasma half-life was unchanged because of a concomitant reduction in volume of distribution (see Table 5).

The indanyl analogues (**78–81**) were synthesized in an attempt to provide compounds with similar rigidity to **49** that presented the key pharmacophores to FTase in a more optimal fashion (vide supra). Both diastereomers were analyzed by NMR spectroscopy and it was found that the resonances in the proton spectrum exhibited negligible line broadening upon cooling from 25 to -50 °C, indicating that the compounds were either highly mobile at all temperatures investigated or quite rigid. For each diastereomer, solution structure data derived from NOESY experiments run at 0 °C indicated that the compounds were highly rigid. This is illustrated in Figure 3 panels E and F for compounds **78** and **80**, respectively. Pharmacokinetic evaluation of **78** and **80** in dogs found that plasma clearance was within 2-fold of that for **49** in both cases, in line with the similar rigidity of the three compounds (see Table 5). Consistent with these low values for CL_p , the compounds possessed improved half-lives with respect to the original lead **11**,

although the volume of distribution was apparently limiting for both compounds (iv $t_{1/2} = 1.7 \text{ h}$ for **78** and 4.2 h for **80**). Thus, the indanyl design of **78** succeeded in terms of both enhancing potency (compare **49** and **78** in Table 4), maintaining a high level of rigidity (Figure 3E), and affording low in vivo clearance (Table 5).

Interestingly, the lowest energy solution structures generated for the highly rigid analogues **49** and **78** were not optimal for binding to the crystallographically determined FTase active site. To superimpose the low-energy solution conformation of **49** with the conformation bound to FTase, it was necessary to rotate the imidazole moiety significantly. If the molecule is oriented as shown in Figure 3C, the imidazole ring points slightly forward, out of the plane of the paper, in the lowest energy conformer. This imidazole must be rotated back, into the plane of the paper, to produce a conformation that resembles that bound to FTase (shown in Figure 2A). A similar adjustment of **78** was also required to dock the compound into the FTase active site. These observations highlight the fact that low-energy solution conformations of a small molecule may be quite different from those that bind to a biological receptor, even when the small molecule is highly rigid. Nonetheless, the stereochemistry of **78** defines the relative orientations of the pyrrolidinone and indane rings, since there is a high energy barrier to rotation of the pyrrolidinone about the N-1–C-1 axis in this system. Thus, when **78** is bound to the active site of FTase, the carbonyl group is presumably oriented as shown in Figure 3E (pointing out of the plane of the paper in this view). In terms of the orientation shown in Figure 2, this means the carbonyl in enzyme-bound **78** would point to the left, away from the catalytic zinc ion, in contrast to the crystal structures of **49** and **66** bound to FTase.

The marked rigidity of **78** in solution, coupled with the fact that it apparently must rearrange in order to bind to FTase, may explain why expansion of the indanyl 5-member ring to give **83** enhanced potency even further. This modification presumably increased the flexibility of the macrocycle and allowed it to bind more optimally to the enzyme, although additional hydrophobic interactions with the added methylene group may also contribute. Unfortunately, while compound **83** and its chromane analogue **85** possessed unique cell potency, they lacked the improvements in terms of plasma clearance and half-life that other analogues had shown (see Table 5). These parameters probably reflected higher rates of metabolic clearance and this may be due in part to increased flexibility, and additional sites for oxidative metabolism, in the homologated ring of compounds such as **83**.

Conclusion

Incorporation of the macrocyclic constraint into 3-aminopyrrolidinone-based FTIs and the subsequent optimization described herein addressed the major concerns associated with the lead compound **1**, by increasing the plasma half-life and decreasing the propensity to prolong the QT_c interval. The majority of these macrocycles had reduced affinity for the hERG potassium channel and this appeared to correlate with minimal effects on

the QT_c interval in vivo. Additionally, most of the macrocycles reported here had improved iv half-lives in dogs compared to **1**. These improvements in half-life were consistently due to reduced plasma clearance and this appeared to correlate with the rigidity of the molecules, a concept that proved useful in inhibitor design. Finally, while the original lead **1** was itself a highly potent FTI, substantial improvements in potency were made, leading to the discovery of the most potent inhibitors of FTase in cells yet described.

Experimental Section

General Methods. Proton NMR spectra were run at 300 MHz on a Varian VXR-300 or at 400 MHz on a Varian Unity 400 or VXR-400 spectrometer, and chemical shifts are reported in parts per million (δ) downfield from tetramethylsilane as internal standard. Fast atom bombardment mass spectra were recorded on a VG-ZAB-HF spectrometer with glycerol as matrix. Electrospray mass spectra were recorded on a Micro-mass ZMD spectrometer. Elemental analyses were performed on a Perkin-Elmer 2400 model II elemental analyzer. Silica gel 60 (230–400 mesh) from EM Science was used for column chromatography, and analytical or preparative thin-layer chromatography was conducted with EM Science Kieselgel 60 F₂₅₄ plates. Thermoseparations HPLC equipment with a Vydac C18 reversed-phase column, or Hewlett-Packard 1100 Series HPLC with a MetaChem Inertsil column, was used for analytical or preparative HPLC. The elution used either a gradient of 95/5 to 0/100 A/B, where A = H₂O–0.1% TFA and B = CH₃CN–0.1% TFA (method A), or a gradient of 95/5 to 5/95 A/B, where A = H₂O–0.1% H₃PO₄ and B = CH₃CN (method B). Enantiomeric purity of final compounds was established by HPLC on either a Chiralpak AD or a Chiralcel OD column. For reactions performed under anhydrous conditions, glassware was either oven- or flame-dried and the reaction was run under a positive pressure of argon. Tetrahydrofuran was freshly distilled from sodium/benzophenone; all other anhydrous solvents were used as purchased from Aldrich. Except where noted, reagents were purchased from Aldrich and used without further purification. The reported yields are the actual isolated yields of purified material and are not optimized.

Synthesis of (20*R*)-19,20,21,22-Tetrahydro-19-oxo-17*H*-18,20-ethano-6,10:12,16-dimetheno-16*H*-imidazo[3,4-*h*]-[1,8,11,14]oxatriazacycloecosine-9-carbonitrile Hydrochloride (11**):** (i) **3-(Benzyloxy)benzyl Azide (**5**)**. To a stirred solution of 3-benzyloxybenzyl alcohol (**4**) (5.0 g, 23.3 mmol) and diphenylphosphoryl azide (7.7 g, 28.0 mmol) in dry toluene (40 mL) at 0 °C was added 1,8-diazabicyclo[5.4.0]-undec-7-ene (3.9 g, 25.6 mmol). The resulting mixture was allowed to warm to ambient temperature and stirred under argon for 18 h and then washed with water (2 × 15 mL) and then 5% hydrochloric acid (15 mL). The organic layer was dried over MgSO₄, filtered, and concentrated in vacuo. The crude product was purified by flash column chromatography on silica, with elution by hexane/4% EtOAc, to yield the product as a colorless oil (5.4 g, 97%): ¹H NMR (CDCl₃) δ 7.45–7.27 (6H, m), 6.97–6.93 (2H, m), 6.91 (1H, d, J = 7.7 Hz), 5.08 (2H, s), 4.31 (2H, s).

(ii) **3-(Benzyloxy)benzylamine (**6**)**. Azide **5** (5.00 g, 20.9 mmol) was dissolved in dry THF (100 mL) and the solution was cooled to –70 °C. LiAlH₄ (31.4 mL of a 1.0 M solution in THF, 31.4 mmol) was added dropwise, and then the reaction mixture was warmed to 0 °C and stirred for 30 min. The reaction was quenched with EtOAc (1.2 mL), then water (1.2 mL), then 15% NaOH (1.2 mL), and finally water (3.6 mL). The resulting mixture was filtered, concentrated under reduced pressure, and purified by flash column chromatography on silica, with elution by CH₂Cl₂/3% MeOH/0.3% NH₄OH, to yield the titled product as a colorless oil (3.87 g, 87%): ¹H NMR (CDCl₃) δ 7.45–7.30 (5H, m), 7.25 (1H, t, J = 7.8 Hz), 6.96 (1H, d, J = 1.6 Hz), 6.91 (1H, dd, J = 7.5, 0.6 Hz), 6.86 (1H,

dd, J = 8.2, 2.2 Hz), 5.07 (2H, s), 3.85 (2H, s), 1.47 (2H, br s); MS (FAB) m/z = 214 (M⁺ + H).

(iii) **(*R*)-2-[(*tert*-Butoxycarbonyl)amino]-4-(methylmercapto)-*N*-[3-(benzyloxy)benzyl]butyramide (**7**)**. To (*R*)-*N*-(*tert*-butoxycarbonyl)methionine (1.20 g, 4.81 mmol) in dry CH₂Cl₂ (25 mL) under argon were added PyBOP (2.90 g, 5.57 mmol), amine **6** (1.00 g, 4.69 mmol), and *N,N*-diisopropylethylamine (0.89 mL, 5.11 mmol). The reaction mixture was stirred for 18 h, then extracted with saturated aqueous NaHCO₃ (25 mL), dried over MgSO₄, filtered, and concentrated in vacuo. The crude product was purified by flash column chromatography on silica, with elution by hexane/25% EtOAc, to yield the product as a white solid (2.04 g, 98%): ¹H NMR (CDCl₃) δ 7.44–7.30 (5H, m), 7.23 (1H, t, J = 7.7 Hz), 6.91–6.83 (3H, m), 6.50 (1H, br s), 5.14 (1H, br s), 5.05 (2H, s), 4.42 (2H, d, J = 5.3 Hz), 4.27 (1H, m), 2.63–2.47 (2H, m), 2.11 (1H, m), 2.08 (3H, s), 1.94 (1H, m), 1.42 (9H, s); MS (FAB) m/z = 445 (M⁺ + H); HPLC purity = 99.5% (method B, 215 nm).

(iv) **(*R*)-1-[3-(Benzyloxy)benzyl]-3-[(*tert*-butoxycarbonyl)amino]-2-oxopyrrolidine (**8**)**. A solution of **7** (2.00 g, 4.50 mmol) in iodomethane (12 mL, 193 mmol) was stirred under argon for 18 h. The iodomethane was removed by distillation under reduced pressure to give (*R*)-2-[(*tert*-butoxycarbonyl)amino]-4-(dimethylsulfoniumyl)-*N*-[3-(benzyloxy)benzyl]butyramide iodide as a yellow solid (2.65 g, 100%): ¹H NMR (CDCl₃) δ 8.26 (1H, br s), 7.46–7.28 (5H, m), 7.21 (1H, t, J = 8.0 Hz), 7.04 (1H, s), 6.96 (1H, d, J = 7.5 Hz), 6.84 (1H, dd, J = 8.1, 1.9 Hz), 6.10 (1H, d, J = 7.0 Hz), 5.08 (2H, s), 4.52 (1H, m), 4.39 (2H, d, J = 6.0 Hz), 3.70 (1H, m), 3.38 (1H, m), 3.20 (3H, s), 2.98 (3H, s), 2.68 (1H, m), 2.12 (1H, m), 1.41 (9H, s); MS (FAB) m/z = 459 (M⁺).

(*R*)-2-[(*tert*-Butoxycarbonyl)amino]-4-(dimethylsulfoniumyl)-*N*-[3-(benzyloxy)benzyl]butyramide iodide (2.60 g, 4.43 mmol) was stirred in dry THF (75 mL), under argon, at 0 °C, and lithium bis(trimethylsilyl)amide (1.0 M in THF, 4.2 mL, 4.2 mmol) was added dropwise. The reaction mixture was stirred at 0 °C for 2 h and then quenched with saturated aqueous NH₄Cl (25 mL), and most of the THF was removed under reduced pressure. The residual solution was partitioned between saturated aqueous NaHCO₃ (25 mL) and CH₂Cl₂ (2 × 25 mL). The combined organic extracts were dried over MgSO₄, filtered, and concentrated in vacuo. The crude product was purified by flash column chromatography on silica, with elution by hexane/40% EtOAc, to yield the titled pyrrolidinone (1.68 g, 96%): ¹H NMR (CDCl₃) δ 7.44–7.29 (5H, m), 7.24 (1H, t, J = 8.1 Hz), 6.91 (1H, dd, J = 7.5, 1.8 Hz), 6.83–6.79 (2H, m), 5.13 (1H, br s), 5.06 (2H, s), 4.48 (1H, d, J = 15.0 Hz), 4.39 (1H, d, J = 14.5 Hz), 4.17 (1H, m), 3.20–3.11 (2H, m), 2.57 (1H, m), 1.79 (1H, ddt, J = 12.5, 10.4, 9.5 Hz), 1.46 (9H, s); MS (FAB) m/z = 397 (M⁺ + H); e.e. = 98.5%.

(v) **(*R*)-3-Amino-1-(3-hydroxybenzyl)-2-oxopyrrolidine Hydrochloride (**9**)**. To a solution of pyrrolidinone **8** (500 mg, 1.26 mmol) in EtOH (75 mL) was added 20% Pd(OH)₂ on carbon (75 mg), and the reaction mixture was stirred under an atmosphere of hydrogen (ca. 1 atm) at ambient temperature for 18 h. The mixture was filtered through a pad of Celite, which was washed with EtOH, and the filtrate was concentrated in vacuo to give a crude product. This was purified by flash column chromatography on silica, with elution by CHCl₃/3% MeOH/0.3% NH₄OH, to yield (*R*)-3-[(*tert*-butoxycarbonyl)amino]-1-(3-hydroxybenzyl)-2-oxopyrrolidine as a colorless oil (357 mg, 92%): ¹H NMR (CDCl₃) δ 7.17 (1H, t, J = 7.8 Hz), 6.79–6.70 (3H, m), 6.56 (1H, br s), 5.23 (1H, d, J = 5.5 Hz), 4.47 (1H, d, J = 14.8 Hz), 4.36 (1H, d, J = 14.5 Hz), 4.32 (1H, m), 3.29–3.19 (2H, m), 2.58 (1H, m), 1.87 (1H, m), 1.42 (9H, s); MS (FAB) m/z = 307 (M⁺ + H); HPLC purity = 97.2% (method B, 215 nm).

A solution of (*R*)-3-[(*tert*-butoxycarbonyl)amino]-1-(3-hydroxybenzyl)-2-oxopyrrolidine (350 mg, 1.14 mmol) in EtOAc (20 mL) at 0 °C was saturated with HCl (g). After 15 min, the mixture was concentrated in vacuo to yield the amine hydrochloride as a white solid (280 mg, 100%): ¹H NMR (CD₃OD) δ 7.16 (1H, td, J = 7.5, 1.1 Hz), 6.76–6.69 (3H, m), 4.46 (1H, d,

$J = 14.7$ Hz), 4.38 (1H, d, $J = 14.6$ Hz), 4.32 (1H, dd, $J = 10.4, 8.9$ Hz), 3.40–3.34 (2H, m), 2.54 (1H, m), 1.97 (1H, m); MS (FAB) $m/z = 207$ ($M^+ + H$); HPLC purity = 98.0% (method B, 215 nm).

(vi) **(R)-2-Fluoro-4-(5-{[1-(3-hydroxybenzyl)-2-oxopyrrolidin-3-ylamino]methyl}imidazol-1-ylmethyl)benzonitrile (10)**. Amine hydrochloride **9** (200 mg, 0.82 mmol) and 1-(4-cyano-3-fluorobenzyl)-5-imidazolecarboxaldehyde⁷ (197 mg, 0.86 mmol) were stirred in MeOH (7 mL), and *N,N*-diisopropylethylamine was added dropwise to adjust the mixture to ca. pH 5, as judged by wetted pH paper. The mixture was stirred for 1 h at ambient temperature; then NaCNBH_3 (54 mg, 0.86 mmol) was added and stirring was continued for 18 h. The reaction was quenched with saturated aqueous NaHCO_3 (2 mL) and most of the MeOH was removed under reduced pressure. The residual solution was partitioned between saturated aqueous NaHCO_3 (3 mL) and CH_2Cl_2 (10 mL). The aqueous layer was extracted further with CH_2Cl_2 (3×10 mL). The combined organic extracts were dried over MgSO_4 , filtered, and concentrated in vacuo. The crude product was purified by flash column chromatography on silica, with elution by two column volumes of EtOAc/10% MeOH, then two column volumes of CHCl_3 /4% MeOH, and then CHCl_3 /4% MeOH/0.4% NH_4OH , to yield the titled product as a colorless oil (261 mg, 76%): ^1H NMR (CDCl_3) δ 7.62–7.56 (2H, m), 7.16 (1H, t, $J = 7.9$ Hz), 7.02–6.97 (2H, m), 6.94 (1H, d, $J = 9.5$ Hz), 6.78 (1H, dd, $J = 7.9, 2.0$ Hz), 6.67 (1H, d, $J = 7.7$ Hz), 6.41 (1H, s), 5.63 (1H, d, $J = 16.7$ Hz), 5.41 (1H, d, $J = 16.7$ Hz), 4.59 (1H, d, $J = 14.6$ Hz), 3.99 (1H, d, $J = 14.6$ Hz), 3.79 (1H, d, $J = 14.5$ Hz), 3.72 (1H, d, $J = 14.5$ Hz), 3.53 (1H, dd, $J = 9.7, 8.4$ Hz), 3.20–3.11 (2H, m), 2.09 (1H, m), 1.80 (1H, m); MS (FAB) $m/z = 420$ ($M^+ + H$); HPLC purity = 100% (method B, 215 nm).

(vii) **(20R)-19,20,21,22-Tetrahydro-19-oxo-17H-18,20-ethano-6,10:12,16-dimetheno-16H-imidazo[3,4-*h*][1,8,11,14]oxatriazacycloicosine-9-carbonitrile Hydrochloride (11)**. A mixture of phenol **10** (200 mg, 0.48 mmol) and Cs_2CO_3 (233 mg, 0.72 mmol) in dry, degassed DMF (4 mL) was stirred at 50 °C under argon for 18 h. Acetic acid (60 μL , 1.0 mmol) was added and the solvent was removed under reduced pressure. The residue was partitioned between saturated aqueous NaHCO_3 (5 mL) and CHCl_3 (10 mL). The aqueous layer was extracted further with CHCl_3 (3×10 mL). The combined organic extracts were dried over MgSO_4 , filtered, and concentrated in vacuo. The crude product was purified by flash column chromatography on silica, with elution by CHCl_3 /4% MeOH/0.4% NH_4OH , to yield the desired product (139 mg, 73%), which was converted to the hydrochloride salt by treatment with HCl in EtOAc: ^1H NMR (CD_3OD) δ 9.43 (1H, d, $J = 1.3$ Hz), 7.85 (1H, d, $J = 8.1$ Hz), 7.79 (1H, s), 7.51 (1H, t, $J = 7.9$ Hz), 7.30–7.23 (3H, m), 7.08 (1H, m), 7.02 (1H, dd, $J = 8.2, 1.6$ Hz), 5.67 (1H, d, $J = 15.7$ Hz), 5.51 (1H, d, $J = 15.7$ Hz), 4.90 (1H, d, $J = 15.2$ Hz), 4.57 (1H, t, $J = 9.6$ Hz), 4.44 (1H, d, $J = 14.5$ Hz), 4.10 (1H, d, $J = 15.0$ Hz), 3.67 (1H, d, $J = 14.7$ Hz), 3.67–3.55 (2H, m), 2.59–2.40 (2H, m); MS (FAB) $m/z = 400$ ($M^+ + H$); HPLC purity = 100% (method B, 215 nm); e.e. = 98.9%; Anal. ($\text{C}_{23}\text{H}_{21}\text{N}_5\text{O}_2 \cdot 1.7\text{HCl} \cdot 1.85\text{H}_2\text{O}$) C, H, N.

Synthesis of (20R)-17-(3-Chlorophenyl)-19,20,21,22-tetrahydro-19-oxo-5H,18H-18,20-ethano-6,10:12,16-dimetheno-16H-imidazo[3,4-*h*][1,8,11,14]oxatriazacycloicosine-9-carbonitrile Hydrochloride, Diastereomer A (27A): (i) **[3-(Benzyloxy)phenyl](3-chlorophenyl)methylamine (18)**. To a stirred suspension of Rieke Mg (Rieke Metals, Inc.) (0.93 g, 38 mmol) in refluxing dry THF (15 mL) under argon was added 1-(benzyloxy)-3-bromobenzene (**17**) (9.00 g, 34.2 mmol) in dry THF (90 mL) dropwise, over 10 min, with the heat source removed. The resulting mixture was heated to reflux for 1 h and then cooled to –12 °C and added dropwise to a stirred solution of 3-chlorobenzaldehyde (4.65 mL, 41.0 mmol) in dry THF (30 mL) at –78 °C. The reaction mixture was stirred at –78 °C for 1 h and then quenched with saturated aqueous NH_4Cl (200 mL) and extracted with Et_2O (500 mL). The organic layer was dried over MgSO_4 , filtered,

and concentrated in vacuo. The residue was purified by silica gel chromatography, with elution by hexane/7% EtOAc, to give the desired product as a colorless oil (6.70 g, 60%): ^1H NMR (CDCl_3) δ 7.42–7.31 (7H, m), 7.28–7.22 (3H, m), 6.99 (1H, m), 6.95 (1H, d, $J = 7.6$ Hz), 6.89 (1H, dd, $J = 8.3, 2.4$ Hz), 5.75 (1H, s), 5.10 (2H, s), 2.45 (1H, br s); MS (ES) $m/z = 407$ ($M - \text{OH}$).

(ii) **[3-(Benzyloxy)phenyl](3-chlorophenyl)methylamine (19)**. By the procedures described for compounds **5** and **6** but with **18** in place of **4**, the titled compound was obtained as a colorless oil (5.20 g, 91%): ^1H NMR (CDCl_3) δ 7.51–7.30 (10H, m), 7.02 (1H, d, $J = 1.8$ Hz), 6.95 (1H, d, $J = 7.7$ Hz), 6.85 (1H, dd, $J = 8.0, 2.1$ Hz) 5.14 (1H, s), 5.04 (2H, s).

(iii) **(3R)-2-[(*tert*-Butoxycarbonyl)amino]-4-(methylmercapto)-*N*-[3-(benzyloxy)phenyl](3-chlorophenyl)methylbutyramide, Diastereomers A and B (20)**. By the procedure described for compound **7** but with **19** in place of **6**, the titled compounds were obtained as a mixture (ca. 1:1 diastereomers) (3.40 g, 99%): ^1H NMR (CDCl_3) δ 7.52–7.29 (5H, m), 7.27–7.21 (4H, m), 7.11 (1H, m), 7.02 (1H, m), 6.89 (1H, m), 6.82 (2H, m), 6.13 (1H, m), 5.12 (1H, br s), 5.02 (2H, s), 4.29 (1H, m), 2.60–2.44 (2H, m), 2.21–1.86 (5H, m), 1.42 (9H, s).

(iv) **(3R)-[1-[3-(Benzyloxy)phenyl](3-chlorophenyl)methyl]-2-oxopyrrolidin-3-yl]carbamic Acid *tert*-Butyl Ester, Diastereomers A and B (21)**. By the procedures described for compound **8** but with **20** in place of **7**, the titled compound was obtained as a mixture (ca. 1:1) of diastereomeric pyrrolidinones (2.40 g, 82%): ^1H NMR (CDCl_3) δ 7.29–7.24 (2H, m), 7.15 (1H, one diastereomer, t, $J = 1.8$ Hz), 7.12 (1H, one diastereomer, m), 7.05 (1H, one diastereomer, dt, $J = 7.0, 1.6$ Hz), 7.03–7.00 (1H, one diastereomer, m), 6.49 (1H, one diastereomer, br s), 6.48 (1H, one diastereomer, br s).

(v) **(3R)-3-Amino-1-[3-(chlorophenyl)(3-hydroxyphenyl)methyl]-2-oxopyrrolidine Trifluoroacetate, Diastereomer A (23A)**. To a solution of ester **21** (2.25 g, 4.52 mmol) in EtOH (125 mL) and EtOAc (75 mL) were added 20% $\text{Pd}(\text{OH})_2$ on carbon (1.0 g) and acetic acid (10 mL), and the reaction mixture was stirred under an atmosphere of hydrogen (ca. 1 atm) at ambient temperature for 4 h. The mixture was filtered through a pad of Celite, which was washed with EtOH, and the filtrate was concentrated in vacuo to give crude (3R)-[1-[3-(chlorophenyl)(3-hydroxyphenyl)methyl]-2-oxopyrrolidin-3-yl]carbamic acid *tert*-butyl ester, diastereomers A and B. This mixture was purified by flash chromatography on silica, with elution by a gradient of CHCl_3 /20–30% EtOAc, to yield the separated products, diastereomer A (higher R_f on silica gel) (275 mg, 15%) [^1H NMR (CDCl_3) δ 7.36–7.07 (5H, m), 6.79 (1H, dd, $J = 7.5, 2.4$ Hz), 6.67–6.63 (2H, m), 6.47 (1H, s)] and diastereomer B (lower R_f on silica gel) (380 mg, 20%) [^1H NMR (CDCl_3) δ 7.37–7.03 (5H, m), 6.80 (1H, m), 6.70–6.66 (2H, m), 6.47 (1H, s)].

A solution of (3R)-[1-[3-(chlorophenyl)(3-hydroxyphenyl)methyl]-2-oxopyrrolidin-3-yl]carbamic acid *tert*-butyl ester, diastereomer A (262 mg, 0.63 mmol), in EtOAc (20 mL) at 0 °C was saturated with HCl (g). After 15 min, the mixture was concentrated in vacuo to yield the amine hydrochloride salt as a white solid. The crude product was purified by preparative HPLC on a Deltapak C-18 column, with elution by a gradient of 0.1% aqueous trifluoroacetic acid/5–60% CH_3CN , to provide the titled product (178 mg, 78%): ^1H NMR (CD_3OD) 7.40–7.34 (2H, m), 7.24–7.08 (2H, m), 6.79 (1H, dd, $J = 7.7, 2.0$ Hz), 6.68 (1H, d, $J = 7.5$ Hz), 6.61 (1H, t, $J = 1.8$ Hz), 6.38 (1H, s), 4.16 (1H, dd, $J = 10.9, 8.5$ Hz), 3.42–3.20 (2H, m), 2.56 (1H, m), 2.06 (1H, m); MS (FAB) $m/z = 317$ (M^+).

(vi) **(3R)-4-{[5-{[1-[3-(Chlorophenyl)(3-hydroxyphenyl)methyl]-2-oxopyrrolidin-3-yl]amino]methyl}imidazol-1-yl]methyl}-2-fluorobenzonitrile, Diastereomer A (25A)**. By the procedure described for compound **10** but with **23A** in place of **9**, the titled compound was obtained as a white solid (123 mg, 83%): ^1H NMR (CDCl_3) δ 7.59 (1H, dd, $J = 8.1, 6.6$ Hz), 7.57 (1H, s), 7.21–7.14 (5H, m), 7.07 (1H, m), 7.04 (1H, s), 7.01 (1H, d, $J = 8.1$ Hz), 6.95 (1H, d, $J = 9.7$ Hz), 6.81 (1H, dd, $J = 8.0, 2.5$ Hz), 6.47 (1H, d, $J = 7.7$ Hz), 6.35 (1H, s), 6.25 (1H, s).

(vii) **(20*R*)-17-(3-Chlorophenyl)-19,20,21,22-tetrahydro-19-oxo-5*H*,18*H*-18,20-ethano-6,10:12,16-dimetheno-16*H*-imidazo[3,4-*h*][1,8,11,14]oxatriazacycloeicosine-9-carbonitrile Hydrochloride, Diastereomer A (27A).** By the procedure described for compound **11** but with **25A** in place of **10** and at a lower concentration (0.03 M), the titled compound was obtained (62 mg, 64%): $^1\text{H NMR}$ (CD_3OD) δ 9.40 (1H, d, $J = 1.1$ Hz), 7.86 (1H, s), 7.79 (1H, d, $J = 8.2$ Hz), 7.53 (1H, t, $J = 8.0$ Hz), 7.41–7.39 (2H, m), 7.35 (1H, s), 7.29–7.21 (3H, m), 7.19 (1H, s), 7.09 (1H, d, $J = 7.7$ Hz), 6.91 (1H, d, $J = 8.1$ Hz), 6.26 (1H, s); MS (FAB) $m/z = 510$ ($\text{M}^+ + \text{H}$); HPLC purity = 98% (method B, 215 nm); e.e. = 99%; Anal. ($\text{C}_{29}\text{H}_{24}\text{ClN}_5\text{O}_2 \cdot 1.9\text{HCl} \cdot 1.6\text{H}_2\text{O}$) C, H, N.

Synthesis of (20*R*)-17-(3-Chlorophenyl)-19,20,21,22-tetrahydro-19-oxo-5*H*,18*H*-18,20-ethano-6,10:12,16-dimetheno-16*H*-imidazo[3,4-*h*][1,8,11,14]oxatriazacycloeicosine-9-carbonitrile Hydrochloride, Diastereomer B (27B): (i) **(3*R*)-4-([1-((3-Chlorophenyl)(3-hydroxyphenyl)methyl)-2-oxopyrrolidin-3-yl]amino)methylimidazol-1-ylmethyl]-2-fluorobenzonitrile, Diastereomer B (25B). By the procedures described for compound **25A** but with (3*R*)-1-[(3-chlorophenyl)(3-hydroxyphenyl)methyl]-2-oxopyrrolidin-3-yl]carbamate *tert*-butyl ester, diastereomer B, in place of (3*R*)-1-[(3-chlorophenyl)(3-hydroxyphenyl)methyl]-2-oxopyrrolidin-3-yl]carbamate *tert*-butyl ester, diastereomer A, the titled compound was obtained (102 mg, 92%) and converted to the hydrochloride salt: $^1\text{H NMR}$ (CD_3OD) δ 9.11 (1H, d, $J = 0.9$ Hz), 7.86 (1H, s), 7.80 (1H, dd, $J = 8.0, 6.7$ Hz), 7.40–7.32 (3H, m), 7.24–7.16 (3H, m), 6.79 (1H, dd, $J = 7.7, 2.0$ Hz), 6.68 (1H, d, $J = 7.5$ Hz), 6.61 (1H, m), 6.40 (1H, s).**

(ii) **(20*R*)-17-(3-Chlorophenyl)-19,20,21,22-tetrahydro-19-oxo-5*H*,18*H*-18,20-ethano-6,10:12,16-dimetheno-16*H*-imidazo[3,4-*h*][1,8,11,14]oxatriazacycloeicosine-9-carbonitrile Hydrochloride, Diastereomer B (27B).** To a solution of phenol **25B** (50.0 mg, 0.094 mmol) in acetonitrile (10 mL) was added KF on alumina (40 wt %, 50 mg) and 18-crown-6 (2.5 mg, 0.6 μmol), and the mixture was heated to reflux for 6 h. The reaction mixture was cooled and filtered, and the solvent was removed under reduced pressure. The crude product was purified by flash chromatography on silica, with elution by a gradient of $\text{CHCl}_3/2\text{--}4\%$ MeOH/ $0.2\text{--}0.4\%$ NH_4OH , to yield the desired product, which was converted to the hydrochloride salt by treatment with HCl in EtOAc (13 mg, 27%): $^1\text{H NMR}$ (CD_3OD) δ 9.31 (1H, s), 7.81 (1H, s), 7.76 (1H, d, $J = 8.1$ Hz), 7.56 (1H, s), 7.50–7.37 (5H, m), 7.24–7.20 (2H, m), 6.82 (1H, d, $J = 8.1$ Hz), 6.64 (1H, d, $J = 8.4$ Hz), 5.75 (1H, s); MS (FAB) $m/z = 510$ ($\text{M}^+ + \text{H}$); HPLC purity = 98% (method B, 215 nm); Anal. ($\text{C}_{29}\text{H}_{24}\text{ClN}_5\text{O}_2 \cdot 2\text{HCl} \cdot 2.1\text{H}_2\text{O} \cdot 0.2\text{EtOAc}$) C, H, N.

Synthesis of (20*R*)-19,20,21,22-Tetrahydro-5-methyl-19-oxo-17*H*,18,20-ethano-6,10:12,16-dimetheno-16*H*-imidazo[3,4-*h*][1,8,11,14]oxatriazacycloeicosine-9-carbonitrile Hydrochloride (36A and 36B): (i) α,α -Dibromo-4-cyano-3-fluorotoluene (29**).** To a solution of 4-cyano-3-fluorotoluene⁷ (**28**) (4.0 g, 29.6 mmol) in carbon tetrachloride (250 mL) was added *N*-bromosuccinimide (10.5 g, 59.2 mmol) and 2,2'-azobis(isobutyronitrile) (490 mg, 3.0 mmol). The reaction mixture was heated to reflux under argon for 24 h and then cooled to room temperature, filtered, and concentrated under reduced pressure. The residue was purified by silica gel chromatography, with elution by a gradient of hexane/3–7% EtOAc, to yield the titled product as a yellow-brown solid (5.62 g, 65%): $^1\text{H NMR}$ (CDCl_3) δ 7.66 (1H, dd, $J = 8.1, 6.4$ Hz), 7.48 (1H, d, $J = 9.2$ Hz), 7.73 (1H, dd, $J = 8.2, 1.3$ Hz), 6.57 (1H, s).

(ii) **4-Cyano-3-fluorobenzaldehyde (30).** To a solution of **29** (5.60 g, 19.1 mmol) in EtOH (255 mL) and water (45 mL) was added AgNO_3 . The mixture was heated to reflux for 3 h, then stood at ambient temperature for 18 h, and then the solid was removed by filtration and the filtrate was concentrated under reduced pressure to a volume of approximately 20 mL. Water (30 mL) was added, and the mixture was concentrated to dryness in vacuo. The residue was partitioned between saturated aqueous NaHCO_3 (20 mL) and CH_2Cl_2 (50 mL). The

aqueous layer was extracted further with CH_2Cl_2 (2×50 mL). The combined organic extracts were dried over Na_2SO_4 , filtered, and concentrated in vacuo. The residue was dried for several days at ca. 0.5 mmHg to yield the desired aldehyde as a pale solid (2.18 g, 77%): $^1\text{H NMR}$ (CDCl_3) δ 10.06 (1H, d, $J = 1.8$ Hz), 7.85 (1H, dd, $J = 7.9, 5.7$ Hz), 7.79 (1H, dd, $J = 7.9, 1.3$ Hz), 7.73 (1H, dd, $J = 8.4, 1.3$ Hz).

(iii) **1-(4-Cyano-3-fluorophenyl)ethanol (31).** To a solution of aldehyde **30** (250 mg, 1.68 mmol) in THF, under argon, at -78°C was added MeMgBr dropwise (3.0 M in Et_2O , 0.59 mL, 1.77 mmol). The reaction mixture was stirred at -78°C for 1 h and then quenched with saturated aqueous NH_4Cl , allowed to warm to ambient temperature, and extracted with CH_2Cl_2 (2×40 mL). The combined organic extracts were dried over Na_2SO_4 , filtered, and concentrated in vacuo. The residue was purified by silica gel chromatography, with elution by a gradient of hexane/20–40% EtOAc, to yield the titled product as a white solid (205 mg, 74%): $^1\text{H NMR}$ (CDCl_3) δ 7.59 (1H, dd, $J = 7.8, 6.5$ Hz), 7.30–7.23 (2H, m), 4.96 (1H, qd, $J = 6.5, 3.9$ Hz), 1.95 (1H, d, $J = 4.0$ Hz), 1.50 (3H, d, $J = 6.6$ Hz).

(iv) **4-[(*tert*-Butyldimethylsilyloxy)methyl]-1-(triphenylmethyl)imidazole (33).** 4-(Hydroxymethyl)-1-(triphenylmethyl)imidazole²¹ (**32**) (1.97 g, 5.72 mmol) and 4-(dimethylamino)pyridine (280 mg, 2.29 mmol) were stirred in CH_2Cl_2 (15 mL), and *tert*-butyldimethylsilyl chloride (905 mg, 6.01 mmol) was added. After 1 min, triethylamine (0.88 mL, 6.31 mmol) was added dropwise over 3 min. The reaction mixture was stirred for 45 min, and then CH_2Cl_2 (150 mL) was added and the solution was washed with 0.1 N HCl (50 mL). The organic layer was dried (Na_2SO_4) and concentrated in vacuo. The residue was purified by silica gel chromatography, with elution by hexane/30% EtOAc, to yield the titled product as a white solid (2.03 g, 78%): $^1\text{H NMR}$ (CDCl_3) δ 7.37 (1H, d, $J = 1.5$ Hz), 7.35–7.29 (9H, m), 7.18–7.12 (6H, m), 6.73 (1H, s), 4.68 (2H, s), 0.85 (9H, s), 0.03 (6H, s).

(v) **5-[(*tert*-Butyldimethylsilyloxy)methyl]-1-[1-(4-cyano-3-fluorophenyl)ethyl]imidazole (34).** A mixture of imidazole **33** (485 mg, 1.07 mmol), alcohol **31** (160 mg, 0.969 mmol), and *N,N*-diisopropylethylamine (0.219 mL, 1.26 mmol) in CH_2Cl_2 (12 mL) was cooled to -78°C , under argon. Trifluoromethanesulfonic anhydride (0.196 mL, 1.17 mmol) was added dropwise, and the mixture was stirred for 18 h while it slowly warmed to ambient temperature. Methanol (15 mL) was added and the CH_2Cl_2 was distilled off in vacuo. The resulting methanolic solution was heated to reflux for 3 h and then concentrated in vacuo to give a residue, which was partitioned between saturated aqueous Na_2CO_3 (10 mL) and CH_2Cl_2 (20 mL). The aqueous layer was extracted further with CH_2Cl_2 (20 mL). The combined organic extracts were dried over Na_2SO_4 , filtered, and concentrated in vacuo. The residue was purified by silica gel chromatography, with elution by a gradient of $\text{CH}_2\text{Cl}_2/0\text{--}5\%$ MeOH, to yield the titled product as a pale foam (319 mg, 92%): $^1\text{H NMR}$ (CDCl_3) δ 7.63 (1H, d, $J = 0.9$ Hz), 7.59 (1H, dd, $J = 8.1, 6.6$ Hz), 6.98 (1H, s), 6.97 (1H, dd, $J = 8.1, 1.5$ Hz), 6.90 (1H, dd, $J = 9.5, 1.5$ Hz), 5.65 (1H, q, $J = 7.1$ Hz), 4.56 (1H, d, $J = 13.4$ Hz), 4.37 (1H, dd, $J = 13.2, 0.6$ Hz), 1.89 (3H, d, $J = 7.3$ Hz), 0.82 (9H, s), 0.01 (3H, s), -0.02 (3H, s).

(vi) **1-[1-(4-Cyano-3-fluorophenyl)ethyl]-5-imidazole-carboxaldehyde (35).** To a solution of imidazole **34** (101 mg, 0.281 mmol) in THF (2 mL) was added TBAF (1.0 M in THF, 0.309 mL, 0.309 mmol), dropwise. The reaction mixture was stirred for 1 h and then poured into saturated aqueous NaHCO_3 (20 mL) and extracted with CH_2Cl_2 (3×20 mL). The combined organic extracts were dried over Na_2SO_4 , filtered, and concentrated in vacuo. The residue was purified by silica gel chromatography, with elution by a gradient of $\text{CH}_2\text{Cl}_2/0\text{--}10\%$ MeOH, to yield 1-[1-(4-cyano-3-fluorophenyl)ethyl]-5-(hydroxymethyl)imidazole as a pale solid (60 mg, 87%): $^1\text{H NMR}$ ($\text{CDCl}_3/\text{CD}_3\text{OD}$) δ 7.69 (1H, s), 7.63 (1H, dd, $J = 8.1, 6.6$ Hz), 7.05 (1H, dd, $J = 8.1, 1.5$ Hz), 6.98 (1H, m), 6.96 (1H, s), 5.72 (1H, q, $J = 7.2$ Hz), 4.50 (1H, d, $J = 13.6$ Hz), 4.26 (1H, d, $J = 13.6$ Hz), 3.56 (1H, br s), 1.90 (3H, d, $J = 7.6$ Hz).

To a solution of 1-[1-(4-cyano-3-fluorophenyl)ethyl]-5-(hy-

droxymethyl)imidazole (60 mg, 0.245 mmol) in dry DMSO (1 mL) was added triethylamine (0.136 mL, 0.979 mmol), followed by SO₃-pyridine complex (97 mg, 0.612 mmol). The reaction mixture was stirred for 30 min and then poured into EtOAc (10 mL), and the organic solution was washed with water (4 × 2 mL), then brine (2 mL), and then dried over Na₂SO₄, filtered, and concentrated in vacuo to yield the desired product as a pale solid (53 mg, 89%): ¹H NMR (CDCl₃) δ 9.68 (1H, d, *J* = 0.9 Hz), 7.98 (1H, s), 7.88 (1H, s), 7.60 (1H, dd, *J* = 8.0, 6.7 Hz), 7.05 (1H, dd, *J* = 8.2, 1.4 Hz), 6.98 (1H, dd, *J* = 9.5, 1.1 Hz), 6.29 (1H, q, *J* = 7.2 Hz), 1.91 (3H, d, *J* = 7.1 Hz).

(vii) (20*R*)-19,20,21,22-Tetrahydro-5-methyl-19-oxo-17*H*-18,20-ethano-6,10:12,16-dimetheno-16*H*-imidazo[3,4-*h*][1,8,11,14]oxatriazacycloecosine-9-carbonitrile Hydrochloride, Diastereomers A and B (36*A* and 36*B*). By the procedures described for compound **11** but with **35** in place of 1-(4-cyano-3-fluorobenzyl)-5-imidazolecarboxaldehyde, the above diastereomers were obtained (53 mg, 55%). The product was obtained as a ca. 1:1 mixture of two diastereomers, which were separated by preparative HPLC on a Chiralpak AS column, with elution by hexane/20% EtOH/20% MeOH/0.1% Et₃NH to yield the separated products, diastereomer A (36*A*) (which eluted first under the described HPLC conditions) and diastereomer B (36*B*) (which eluted second under the described HPLC conditions).

(20*R*)-19,20,21,22-Tetrahydro-5-methyl-19-oxo-17*H*-18,20-ethano-6,10:12,16-dimetheno-16*H*-imidazo[3,4-*h*][1,8,11,14]oxatriazacycloecosine-9-carbonitrile, Diastereomer A (36*A*): ¹H NMR (CDCl₃) δ 5.47 (1H, q, *J* = 7.3 Hz), 1.76 (3H, d, *J* = 7.3 Hz). This was converted to the hydrochloride salt by treatment with HCl in EtOAc: MS (FAB) *m/z* = 414 (M⁺ + H); HPLC purity = 97.1% (method B, 215 nm); Anal. (C₂₄H₂₃N₅O₂·2HCl·0.85H₂O·0.3EtOAc) C, H, N.

(20*R*)-19,20,21,22-Tetrahydro-5-methyl-19-oxo-17*H*-18,20-ethano-6,10:12,16-dimetheno-16*H*-imidazo[3,4-*h*][1,8,11,14]oxatriazacycloecosine-9-carbonitrile, Diastereomer B (36*B*): ¹H NMR (CDCl₃) δ 5.50 (1H, q, *J* = 7.2 Hz), 1.80 (3H, d, *J* = 7.1 Hz). This was converted to the hydrochloride salt by treatment with HCl in EtOAc: MS (FAB) *m/z* = 414 (M⁺ + H); HPLC purity = 99.3% (method B, 215 nm); Anal. (C₂₄H₂₃N₅O₂·2HCl·1.05H₂O·0.5EtOAc) C, H, N.

Synthesis of (23*R*)-22,23,24,25-Tetrahydro-22-oxo-16*H*,21*H*-21,23-ethano-6,10:12,16-dimethenobenz[*g*]-imidazo[4,3-*n*][1,9,12,15]oxatriazacycloheneicosine-9-carbonitrile Hydrochloride (42): (i) 2-(3-Methoxyphenyl)-nitrobenzene (39). A mixture of (3-methoxyphenyl)boronic acid (7.4 g, 48.7 mmol), 2-bromonitrobenzene (**38**) (10.3 g, 40.6 mmol), and K₂CO₃ (28.1 g, 202.9 mmol) was dissolved in H₂O (85 mL) and ethylene glycol dimethyl ether (170 mL). The solution was degassed, then Pd(PPh₃)₄ (1.7 g, 1.50 mmol) was added, and the reaction mixture was heated to 110 °C, under argon, for 5 h. The reaction mixture was cooled and then partitioned between dilute NaHCO₃ (100 mL) and Et₂O (150 mL). The aqueous layer was extracted further with Et₂O (2 × 150 mL). The combined organic extracts were dried over Na₂SO₄, filtered, and concentrated in vacuo. The crude product was dissolved in hot EtOAc/hexane and filtered, and the filtrate was concentrated in vacuo and purified by flash column chromatography on silica, with elution by a gradient of hexane/1–10% EtOAc, to yield the desired product as a crystalline solid (8.65 g, 93%): ¹H NMR (CDCl₃) δ 7.84 (1H, d, *J* = 7.1 Hz), 7.62 (1H, td, *J* = 7.5, 1.1 Hz), 7.51–7.44 (2H, m), 7.47 (1H, t, *J* = 7.8 Hz), 6.96–6.86 (3H, m), 3.83 (3H, s).

(ii) 2-(3-Hydroxyphenyl)nitrobenzene (40). To a solution of **39** (8.60 g, 37.5 mmol) in CH₂Cl₂ (400 mL) at –78 °C was added BBr₃ (1.0 M in CH₂Cl₂, 43 mL, 43 mmol) dropwise. The reaction mixture was allowed to warm to ambient temperature and stirred for 18 h. The reaction mixture was quenched with saturated aqueous NaHCO₃ (100 mL) and extracted with CH₂Cl₂ (3 × 150 mL). The combined organic extracts were dried over Na₂SO₄, filtered, and concentrated in vacuo to yield the titled compound (8.64 g, 98%): ¹H NMR (CDCl₃) δ 7.83 (1H, dd, *J* = 8.1, 1.2 Hz), 7.60 (1H, td, *J* = 7.7, 1.5 Hz), 7.47 (1H,

td, *J* = 7.8, 1.5 Hz), 7.41 (1H, dd, *J* = 7.6, 1.5 Hz), 7.27 (1H, t, *J* = 7.8 Hz), 6.88–6.84 (2H, m), 6.80–6.79 (1H, m).

(iii) 2-[3-[(*tert*-Butyldimethylsilyl)oxy]phenyl]aniline (41). A mixture of phenol **40** (8.07 g, 37.5 mmol), *tert*-butyldimethylsilyl chloride (6.22 g, 41.27 mmol), and imidazole (7.66 g, 112.6 mmol) in dry, degassed DMF (30 mL) was stirred, under argon, at ambient temperature for 45 min. The solvent was removed under reduced pressure and the residue was partitioned between H₂O (100 mL) and Et₂O (200 mL). The aqueous layer was extracted further with Et₂O (2 × 100 mL) and the combined organic extracts were dried over Na₂SO₄, filtered, and concentrated in vacuo. The crude product was purified by flash column chromatography on silica, with elution by a gradient of hexane/0–4% EtOAc, to yield 2-[3-[(*tert*-butyldimethylsilyl)oxy]phenyl]nitrobenzene (11.9 g, 97%).

To a solution of 2-[3-[(*tert*-butyldimethylsilyl)oxy]phenyl]nitrobenzene (11.9 g, 36.2 mmol) in EtOH (250 mL) and EtOAc (250 mL) was added Pd/C (1.19 g, 10 wt %). The reaction mixture was stirred under an atmosphere of hydrogen (ca. 1 atm) at ambient temperature for 2.5 h. The mixture was filtered through a pad of Celite, which was washed with EtOH, and the filtrate was concentrated in vacuo to give the desired product as a brown oil (10.8 g, 99%): ¹H NMR (CDCl₃) δ 7.29 (1H, t, *J* = 7.9 Hz), 7.17–7.11 (2H, m), 6.91 (1H, dt, *J* = 7.6, 1.3 Hz), 6.94 (1H, t, *J* = 2.0 Hz), 6.84–6.79 (2H, m), 6.76 (1H, dd, *J* = 8.0, 1.1 Hz).

(iv) (23*R*)-22,23,24,25-Tetrahydro-22-oxo-16*H*,21*H*-21,23-ethano-6,10:12,16-dimethenobenz[*g*]imidazo[4,3-*n*][1,9,12,15]oxatriazacycloheneicosine-9-carbonitrile Hydrochloride (42). By the procedures described for compound **49** but with **41** in place of **44** and (*R*)-*N*-(*tert*-butoxycarbonyl)-methionine in place of (*S*)-*N*-(*tert*-butoxycarbonyl)-methionine, the above compound was obtained (217 mg, 72%): ¹H NMR (CD₃OD) δ 9.22 (1H, s), 7.81 (1H, d, *J* = 7.9 Hz), 7.74 (1H, s), 7.58–7.46 (5H, m), 7.35 (1H, d, *J* = 7.9 Hz), 7.27 (1H, s), 7.23–7.12 (3H, m), 5.57 (2H, s), 4.28 (2H, m), 3.84 (3H, m), 2.55 (1H, m), 2.02 (1H, m); MS (FAB) *m/z* = 462 (M⁺ + H); HPLC purity = 99.6% (method B, 215 nm); Anal. (C₂₈H₂₅N₅O₂·2HCl·2.2H₂O·0.15EtOAc) C, H, N.

Synthesis of (20*S*)-19,20,21,22-Tetrahydro-19-oxo-5*H*-18,20-ethano-12,14-etheno-6,10-metheno-18*H*-benz[*d*]-imidazo[4,3-*k*][1,6,9,12]oxatriazacyclooctadecosine-9-carbonitrile Hydrochloride (49): (i) 1-Amino-7-[(*tert*-butyldimethylsilyl)oxy]naphthalene Hydrochloride (44). A mixture of 8-amino-2-naphthol (**43**) (50.6 g, 0.318 mol) and di-*tert*-butyl dicarbonate (72.8 g, 0.334 mol) in CH₂Cl₂ (1.4 L) and THF (1 L) was heated to reflux for 36 h. The mixture was allowed to cool to ambient temperature and then filtered and concentrated in vacuo. The residue was purified by flash column chromatography on silica, with elution by a gradient of CH₂Cl₂/0–10% EtOAc, to yield 8-[(*tert*-butoxycarbonyl)-amino]-2-naphthol as a light brown solid (77.3 g, 94%): ¹H NMR (CDCl₃) δ 7.76 (1H, br s), 7.74 (1H, d, *J* = 8.9 Hz), 7.58 (1H, d, *J* = 8.2 Hz), 7.31 (1H, t, *J* = 7.9 Hz), 7.18 (1H, d, *J* = 2.4 Hz), 7.07 (1H, dd, *J* = 8.9, 2.4 Hz), 6.59 (1H, br s), 1.56 (9H, s); HPLC purity = 100% (method B, 215 nm).

A mixture of 8-[(*tert*-butoxycarbonyl)amino]-2-naphthol (43.2 g, 0.167 mol), *tert*-butyldimethylsilyl chloride (32.7 g, 0.217 mol), and imidazole (25.0 g, 0.367 mol) in dry, degassed DMF (400 mL) was stirred, under argon, at ambient temperature for 30 min. The solvent was removed under reduced pressure and the residue was partitioned between H₂O (1 L) and Et₂O (2 L). The aqueous layer was extracted further with Et₂O (1 L) and the combined organic extracts were dried over Na₂SO₄, filtered, and concentrated in vacuo. The crude product was purified by flash column chromatography on silica, with elution by hexane/50% CH₂Cl₂, to yield 1-[(*tert*-butoxycarbonyl)amino]-7-[(*tert*-butyldimethylsilyl)oxy]naphthalene as a pale solid (60.5 g, 97%): ¹H NMR (CDCl₃) δ 7.78–7.71 (2H, m), 7.58 (1H, d, *J* = 8.3 Hz), 7.31 (1H, t, *J* = 7.9 Hz), 7.20 (1H, d, *J* = 2.2 Hz), 7.08 (1H, dd, *J* = 8.8, 2.2 Hz), 6.57 (1H, br s), 1.58 (9H, s), 1.03 (9H, s), 0.26 (6H, s).

A solution of 1-[(*tert*-butoxycarbonyl)amino]-7-[(*tert*-butyldimethylsilyl)oxy]naphthalene (28.8 g, 77 mmol) in EtOAc

(1 L) at ambient temperature was saturated with HCl (g). After 30 min, the mixture was concentrated in vacuo to yield the desired product as a pale solid (22.7 g, 95%): ^1H NMR (CD_3OD) δ 7.98–7.94 (2H, m), 7.56 (1H, dd, J = 7.4, 1.1 Hz), 7.43 (1H, dd, J = 7.4, 8.2 Hz), 7.34 (1H, d, J = 2.2 Hz), 7.27 (1H, dd, J = 8.8, 2.2 Hz), 6.57 (1H, br s), 1.06 (9H, s), 0.32 (6H, s).

(ii) **(S)-2-[(*tert*-Butoxycarbonyl)amino]-4-(methylmercapto)-*N*-[7-[(*tert*-butyldimethylsilyl)oxy]naphthalen-1-yl]butyramide (45).** By the procedure for compound **7** but with **44** in place of **6** and (*S*)-*N*-(*tert*-butoxycarbonyl)methionine in place of (*R*)-*N*-(*tert*-butoxycarbonyl)methionine, the titled product was obtained (42.8 g, 85%): ^1H NMR (CDCl_3) δ 8.59 (1H, br s), 8.00 (1H, d, J = 7.4 Hz), 7.74 (1H, d, J = 8.9 Hz), 7.62 (1H, d, J = 8.1 Hz), 7.35–7.28 (2H, m), 7.09 (1H, dd, J = 8.8, 2.2 Hz), 5.27 (1H, br d, J = 6.6 Hz), 4.56 (1H, q, J = 7.0 Hz), 2.76–2.63 (2H, m), 2.31 (1H, m), 2.16 (3H, s), 2.10 (1H, m), 1.03 (9H, s), 0.28 (3H, s), 0.26 (3H, s).

(iii) **(S)-3-[(*tert*-Butoxycarbonyl)amino]-1-[7-[(*tert*-butyldimethylsilyl)oxy]naphthalen-1-yl]-2-oxopyrrolidine (46).** By the procedures for compound **8** but with **45** in place of **7**, the titled product was obtained as a white solid (27 g, 76%): ^1H NMR (CDCl_3) δ 7.80–7.77 (2H, m), 7.36 (1H, t, J = 7.5 Hz), 7.32 (1H, dd, J = 7.2, 1.6 Hz), 7.11 (1H, dd, J = 8.9, 2.4 Hz), 7.00 (1H, d, J = 1.5 Hz), 5.31 (1H, br s), 4.46 (1H, m), 3.84 (1H, td, J = 10.2, 6.2 Hz), 3.72 (1H, t, J = 9.1 Hz), 2.92 (1H, m), 2.22 (1H, m), 1.49 (9H, s), 1.01 (9H, s), 0.25 (6H, s); e.e. = 99.0%.

(iv) **(S)-3-Amino-1-(7-hydroxynaphthalen-1-yl)-2-oxopyrrolidine Hydrochloride (47).** A solution of pyrrolidinone **46** (1.77 g, 3.88 mmol) in EtOAc (150 mL) was cooled to 0 °C and saturated with HCl (g). The reaction was monitored by HPLC until complete conversion had occurred, and then the mixture was concentrated in vacuo to provide the titled product as a white solid: ^1H NMR (CD_3OD) δ 7.84 (2H, d, J = 8.8 Hz), 7.41–7.31 (2H, m), 7.17 (1H, d, J = 8.8 Hz), 7.07 (1H, s), 4.44 (1H, t, J = 9.6 Hz), 4.01 (1H, m), 3.87 (1H, t, J = 9.6 Hz), 2.81 (1H, m), 2.42 (1H, m).

(v) **(S)-2-Fluoro-4-[(5-[[1-(7-hydroxynaphthalen-1-yl)-2-oxopyrrolidin-3-yl]amino]methyl]imidazol-1-yl]methyl]benzonitrile (48).** By the procedure for compound **10** but with **47** in place of **9**, the titled compound was obtained as a pale solid (1.35 g, 96%): ^1H NMR (CDCl_3) δ 7.73 (1H, d, J = 8.8 Hz), 7.70 (1H, d, J = 8.1 Hz), 7.61–7.56 (2H, m), 7.26–7.21 (3H, m), 7.15 (1H, d, J = 8.6 Hz), 7.14 (1H, d, J = 8.8 Hz), 7.00 (1H, d, J = 8.1 Hz), 6.94 (1H, d, J = 9.9 Hz), 6.41 (1H, br s), 5.94 (1H, br d), 5.34 (1H, d, J = 16.8 Hz), 4.08 (1H, m), 3.85 (1H, m), 3.77 (1H, td, J = 10.1, 6.7 Hz), 3.71 (1H, d, J = 14.7 Hz), 3.59 (1H, t, J = 9.2 Hz), 2.50 (1H, m), 2.27 (1H, m).

(vi) **(20S)-19,20,21,22-Tetrahydro-19-oxo-5H-18,20-ethano-12,14-etheno-6,10-metheno-18H-benz[*d*]imidazo[4,3-*k*][1,6,9,12]oxatriazacyclooctadecosine-9-carbonitrile Hydrochloride (49).** By the procedure described for compound **11** but with **48** in place of **10** and at a lower concentration (0.01 M), the titled compound was obtained (1.08 g, 84%): ^1H NMR (CD_3OD) δ 9.49 (1H, d, J = 1.3 Hz), 8.10 (1H, d, J = 9.0 Hz), 8.04 (1H, d, J = 1.3 Hz), 8.01 (1H, s), 7.98 (1H, m), 7.82 (1H, d, J = 8.2 Hz), 7.69 (1H, d, J = 2.2 Hz), 7.59–7.56 (2H, m), 7.53 (1H, dd, J = 9.0, 2.6 Hz), 6.82 (1H, d, J = 8.4 Hz), 5.92 (1H, d, J = 16.1 Hz), 5.52 (1H, d, J = 16.3 Hz), 4.78 (1H, dd, J = 11.4, 9.4 Hz), 4.65 (1H, d, J = 14.7 Hz), 4.35 (1H, m), 3.82 (1H, t, J = 7.8 Hz), 3.70 (1H, d, J = 14.1 Hz), 2.71 (2H, m); MS (FAB) m/z = 436 (M^+ + H); HPLC purity = 100% (method B, 215 nm); e.e. = 99.3%; Anal. ($\text{C}_{26}\text{H}_{21}\text{N}_5\text{O}_2 \cdot 2\text{HCl} \cdot 1.35\text{H}_2\text{O} \cdot 0.4\text{CH}_2\text{Cl}_2$) C, H, N.

Synthesis of (20S)-19,20,22,23-Tetrahydro-19,22-dioxo-5H,21H-18,20-ethano-12,14-etheno-6,10-methenobenz[*d*]imidazo[4,3-*l*][1,6,9,13]oxatriazacyclononadecosine-9-carbonitrile Hydrochloride (56): (i) **Lithium 1-(4-cyano-3-fluorobenzyl)-1H-imidazol-5-yl]acetate (54).** A mixture of methyl [1-(triphenylmethyl)-1H-imidazol-4-yl]acetate⁸ (**52**) (536 mg, 1.40 mmol) and 4-cyano-3-fluorobenzyl bromide⁷ (**53**) (300 mg, 1.40 mmol) in acetonitrile (3 mL) was heated to 50 °C for 2 h. The mixture was allowed to cool, and the solid was

collected by filtration. The acetonitrile filtrate was concentrated in vacuo to a volume of approximately 1 mL and then reheated to 50 °C for 2 h and cooled, and the solid was removed by filtration. The two crops of precipitated imidazolium salts were combined in MeOH (30 mL) and the solution was heated to reflux for 2 h and then concentrated in vacuo. The residue was partitioned between saturated aqueous NaHCO_3 (20 mL) and CHCl_3 (30 mL). The aqueous layer was extracted further with CHCl_3 (2 \times 15 mL). The combined organic extracts were dried over Na_2SO_4 , filtered, and concentrated in vacuo. The crude product was purified by flash column chromatography on silica, with elution by CHCl_3 /3% MeOH/0.3% NH_4OH to CHCl_3 /5% MeOH/0.5% NH_4OH , to yield methyl [1-(4-cyano-3-fluorobenzyl)-1H-imidazol-5-yl]acetate hydrobromide as a white solid (380 mg, 77%): ^1H NMR (CD_3OD) δ 9.03 (1H, s), 7.84 (1H, dd, J = 6.8, 6.8 Hz), 7.61 (1H, s), 7.36 (1H, d, J = 8.0 Hz), 7.30 (1H, d, J = 8.0 Hz), 5.59 (2H, s), 3.89 (2H, s), 3.66 (3H, s).

Methyl [1-(4-cyanobenzyl)-1H-imidazol-5-yl]acetate (free base) (260 mg, 0.95 mmol) was dissolved in THF (5 mL) and H_2O (1 mL). Lithium hydroxide (40 mg, 0.95 mmol) was added and the resulting mixture was stirred at ambient temperature for 1 h, then adjusted to pH 7 with 1.0 N aqueous HCl, and concentrated to dryness in vacuo to give the titled lithium salt:

^1H NMR (CDCl_3) δ 7.71 (1H, s), 7.66 (1H, dd, J = 6.8, 6.6 Hz), 7.46 (1H, s), 7.06 (1H, d, J = 7.9 Hz), 7.00 (1H, d, J = 10.3 Hz), 5.34 (2H, s), 3.43 (2H, s).

(ii) **(S)-2-[1-(4-Cyano-3-fluorobenzyl)-1H-imidazol-5-yl]-*N*-[1-(7-hydroxynaphthalen-1-yl)-2-oxopyrrolidin-3-yl]acetamide (55).** A mixture of **54** (46 mg, 0.18 mmol), **47** (45 mg, 0.16 mmol), HOBT (24 mg, 0.18 mmol), EDC (35 mg, 0.18 mmol), and *N,N*-diisopropylethylamine (0.084 mL, 0.48 mmol) was stirred in DMF (1 mL) at ambient temperature for 18 h. The solvent was removed under reduced pressure and the residue was partitioned between saturated aqueous NaHCO_3 (1 mL) and CHCl_3 (2 mL). The aqueous layer was extracted further with CHCl_3 (2 \times 2 mL). The combined organic extracts were dried over MgSO_4 , filtered, and concentrated in vacuo. The crude product was purified by flash column chromatography on silica, with elution by a gradient of EtOAc/10% MeOH/1% NH_4OH to EtOAc/15% MeOH/1.5% NH_4OH , to yield the titled product as a white solid (54 mg, 69%): ^1H NMR (CD_3OD) δ 7.76–7.69 (3H, m), 7.49 (1H, s), 7.44 (1H, br t), 7.29–7.22 (3H, m), 7.09 (2H, d, J = 7.9 Hz), 6.97 (1H, br s), 6.80 (1H, br s), 6.73 (1H, d, J = 7.9 Hz), 5.13 (2H, br s), 4.62 (1H, s), 3.75 (1H, dd, J = 16.6, 9.2 Hz), 3.63 (1H, t, J = 9.4 Hz), 3.34 (2H, m), 2.47 (1H, m), 2.13 (1H, m); MS (FAB) m/z = 484 (M^+ + H).

(iii) **(20S)-19,20,22,23-Tetrahydro-19,22-dioxo-5H,21H-18,20-ethano-12,14-etheno-6,10-methenobenz[*d*]imidazo[4,3-*l*][1,6,9,13]oxatriazacyclononadecosine-9-carbonitrile Hydrochloride (56).** A mixture of phenol **55** (35 mg, 0.072 mmol) and Cs_2CO_3 (31 mg, 0.095 mmol) in dry DMSO (7 mL) was stirred at ambient temperature, under argon, for 18 h. Acetic acid (0.06 mL, 1.0 mmol) was added and the solvent was removed under reduced pressure. The residue was partitioned between saturated aqueous NaHCO_3 (1 mL) and CHCl_3 (3 mL). The aqueous layer was extracted further with CHCl_3 (2 \times 2 mL). The combined organic extracts were dried over MgSO_4 , filtered, and concentrated in vacuo. The crude product was purified by flash column chromatography on silica, with elution by CHCl_3 /7% MeOH/0.7% NH_4OH , to yield the desired product, which was converted to the hydrochloride salt by treatment with HCl in EtOAc (28 mg, 83%): ^1H NMR (CD_3OD) δ 9.08 (1H, s), 8.06 (1H, d, J = 9.0 Hz), 7.93 (1H, d, J = 8.1 Hz), 7.79 (1H, d, J = 8.0 Hz), 7.71 (1H, s), 7.58 (2H, s), 7.55–7.47 (3H, m), 6.83 (1H, d, J = 8.3 Hz), 5.67 (2H, m), 4.61 (1H, t, J = 9.4 Hz), 4.12 (1H, m), 4.04 (1H, d, J = 17.2 Hz), 3.71 (1H, t, J = 8.9 Hz), 3.29 (1H, m), 2.60 (1H, m), 2.21 (1H, m); MS (FAB) m/z = 464 (M^+ + H); HPLC purity = 96.4% (method B, 215 nm); Anal. ($\text{C}_{27}\text{H}_{21}\text{N}_5\text{O}_3 \cdot \text{HCl} \cdot 2.5\text{H}_2\text{O}$) C, H, N.

Synthesis of (20S)-19,20,22,23-Tetrahydro-19-oxo-5H,21H-18,20-ethano-12,14-etheno-6,10-methenobenz[*d*]-

imidazo[4,3-*f*][1,6,9,13]oxatriazacyclononadecosine-9-carbonitrile Hydrochloride (66): (i) **Lithium [1-(Triphenylmethyl)-1*H*-imidazol-4-yl]acetate (59).** To a solution of ester **52** (1.14 g, 2.98 mmol) in THF (20 mL) and H₂O (3.3 mL) was added lithium hydroxide (1.0 N aqueous, 3.3 mL, 3.3 mmol), and the resulting mixture was stirred at ambient temperature for 18 h, then adjusted to pH 7 with 1.0 N aqueous HCl, and concentrated to dryness in vacuo to give the titled lithium salt as a white solid (1.12 g, 100%): ¹H NMR (CD₃OD) δ 7.39–7.33 (9H, m), 7.31 (1H, d, *J* = 1.5 Hz), 7.19–7.15 (6H, m), 6.84 (1H, s), 3.43 (2H, s).

(ii) **(S)-3-Amino-1-[7-[(*tert*-butyldiphenylsilyl)oxy]naphthalen-1-yl]-2-oxopyrrolidine (58).** To a stirred solution of silyl ether **46** (1.00 g, 2.19 mmol) in THF (5 mL) was added TBAF (1.0 M in THF, 2.4 mL, 2.4 mmol), dropwise, and the resulting mixture was stirred at ambient temperature for 15 min. The reaction mixture was partitioned between saturated aqueous NaHCO₃ (5 mL) and EtOAc (10 mL). The aqueous layer was extracted further with EtOAc (10 mL). The combined organic extracts were dried over MgSO₄, filtered, and concentrated in vacuo. The crude product was purified by flash column chromatography on silica, with elution by hexane/50% EtOAc, to yield (S)-3-[(*tert*-butoxycarbonyl)amino]-1-(7-hydroxynaphthalen-1-yl)-2-oxopyrrolidine (740 mg, 99%): ¹H NMR (CDCl₃) δ 7.74 (1H, t, *J* = 4.7 Hz), 7.66 (1H, d, *J* = 9.2 Hz), 7.31–7.28 (2H, m), 6.98–6.86 (2H, m), 5.56 (1H, br s), 4.61 (1H, m), 3.83 (1H, td, *J* = 9.8, 6.4 Hz), 3.72 (1H, t, *J* = 9.5 Hz), 2.79 (1H, m), 2.31 (1H, m), 1.46 (9H, s).

A stirred mixture of (S)-3-[(*tert*-butoxycarbonyl)amino]-1-(7-hydroxynaphthalen-1-yl)-2-oxopyrrolidine (700 mg, 2.04 mmol), *tert*-butyldiphenylsilyl chloride (1.40 g, 5.09 mmol), and imidazole (418 mg, 6.14 mmol) in dry, degassed DMF (10 mL) was heated at 60 °C for 3 h, and then the solvent was removed under reduced pressure. The crude oil was purified by flash column chromatography on silica, with elution by a gradient of hexane/20–30% EtOAc, to yield (S)-3-[(*tert*-butoxycarbonyl)amino]-1-[7-[(*tert*-butyldiphenylsilyl)oxy]naphthalen-1-yl]-2-oxopyrrolidine as a white solid (1.05 g, 88%): ¹H NMR (CDCl₃) δ 7.79–7.70 (6H, m), 7.47–7.24 (8H, m), 7.16 (1H, d, *J* = 7.1 Hz), 6.63 (1H, d, *J* = 2.1 Hz), 4.82 (1H, br s), 4.13 (1H, m), 3.22 (1H, td, *J* = 9.4, 6.9 Hz), 3.01 (1H, t, *J* = 9.2 Hz), 2.49 (1H, m), 1.49 (1H, m), 1.54 (9H, s), 1.12 (9H, s).

(S)-3-[(*tert*-Butoxycarbonyl)amino]-1-[7-[(*tert*-butyldiphenylsilyl)oxy]naphthalen-1-yl]-2-oxopyrrolidine (1.00 g, 1.72 mmol) was stirred in CH₂Cl₂ (5 mL) and TFA (5 mL) for 30 min at ambient temperature. The reaction mixture was partitioned between saturated aqueous Na₂CO₃ (50 mL) and CH₂Cl₂ (50 mL). The aqueous layer was extracted further with CH₂Cl₂ (2 × 25 mL). The combined organic extracts were dried over MgSO₄, filtered, and concentrated in vacuo to afford the titled product as a white solid (820 mg, 99%): ¹H NMR (CDCl₃) δ 7.80–7.70 (6H, m), 7.45–7.24 (8H, m), 7.16 (1H, dd, *J* = 7.2, 1.0 Hz), 6.63 (1H, d, *J* = 2.3 Hz), 3.26 (1H, t, *J* = 9.0 Hz), 3.14 (1H, td, *J* = 9.6, 6.6 Hz), 3.01 (1H, t, *J* = 9.1 Hz), 2.23 (1H, m), 1.42 (1H, m), 1.12 (9H, s).

(iii) **(S)-*N*-[1-[7-[(*tert*-Butyldiphenylsilyl)oxy]naphthalen-1-yl]-2-oxopyrrolidin-3-yl]-2-[1-(triphenylmethyl)-1*H*-imidazol-4-yl]acetamide (60).** By the procedure for compound **55** but with **59** in place of **54** and **58** in place of **47**, the titled product was obtained (20.5 g, 55%): ¹H NMR (CDCl₃) δ 7.76–7.68 (6H, m), 7.52 (1H, d, *J* = 5.2 Hz), 7.44 (1H, d, *J* = 1.3 Hz), 7.43–7.25 (16H, m), 7.23–7.18 (2H, m), 7.16–7.10 (6H, m), 6.75–6.72 (2H, m), 4.20 (1H, m), 3.61 (1H, d, *J* = 16.9 Hz), 3.55 (1H, d, *J* = 16.9 Hz), 3.23–3.14 (2H, m), 2.55 (1H, m), 1.65 (1H, m), 1.12 (9H, s).

(iv) **(S)-*N*-[1-[7-[(*tert*-Butyldiphenylsilyl)oxy]naphthalen-1-yl]-2-oxopyrrolidin-3-yl]-2-[1-(triphenylmethyl)-1*H*-imidazol-4-yl]thioacetamide (61).** A mixture of amide **60** (17.7 g, 21.3 mmol) and Lawesson's reagent (4.30 g, 10.6 mmol) in dry THF (300 mL) was heated to 45 °C for 15 h. The solvent was removed under reduced pressure and the residue was purified by flash column chromatography on silica, with elution by hexane/40% EtOAc/0.1% NH₄OH, to yield the desired product (7.80 g, 43%): ¹H NMR (CDCl₃) δ 9.90 (1H, d,

J = 5.1 Hz), 7.77–7.68 (6H, m), 7.45 (1H, d, *J* = 1.3 Hz), 7.44–7.25 (16H, m), 7.25–7.19 (2H, m), 7.16–7.09 (6H, m), 6.73 (1H, d, *J* = 1.2 Hz), 6.70 (1H, d, *J* = 2.2 Hz), 4.65 (1H, m), 4.12 (1H, d, *J* = 17.4 Hz), 4.05 (1H, d, *J* = 17.4 Hz), 3.22–3.13 (2H, m), 2.94 (1H, m), 1.65 (1H, m), 1.12 (9H, s).

(v) **(S)-{1-[7-[(*tert*-Butyldiphenylsilyl)oxy]naphthalen-1-yl]-2-oxopyrrolidin-3-yl}-2-[1-(triphenylmethyl)-1*H*-imidazol-4-yl]ethyl} carbamic Acid *tert*-Butyl Ester (62).** To a stirred mixture of thioamide **61** (3.00 g, 3.54 mmol) and NiCl₂·6H₂O (2.50 g, 10.5 mmol) in MeOH (60 mL) and THF (60 mL), at –10 °C, was added NaBH₄ (536 mg, 14.2 mmol) in portions over 30 min, with the reaction temperature kept below –5 °C. The reaction was quenched with saturated aqueous NaHCO₃ (20 mL), the organic solvents were evaporated under reduced pressure, and the residue was partitioned between saturated aqueous Na₂CO₃ (30 mL) and CH₂Cl₂ (50 mL). The aqueous layer was extracted further with CH₂Cl₂ (50 mL) and the combined organic extracts were washed with 0.1 M aqueous EDTA (50 mL), then H₂O (50 mL), and then dried over MgSO₄, filtered, and concentrated in vacuo. The crude product was purified by flash column chromatography on silica, with elution by CH₂Cl₂/1% MeOH/0.1% NH₄OH, to yield (S)-1-[7-[(*tert*-butyldiphenylsilyl)oxy]naphthalen-1-yl]-2-oxo-3-[(2-[1-(triphenylmethyl)-1*H*-imidazol-4-yl]ethyl)amino]pyrrolidine (1.50 g, 52%): ¹H NMR (CDCl₃) δ 7.75–7.68 (6H, m), 7.44–7.24 (16H, m), 7.22–7.11 (9H, m), 6.76 (1H, s), 6.65 (1H, s), 3.26–3.07 (3H, m), 3.04–2.70 (4H, m), 2.13 (1H, m), 1.75 (1H, m), 1.12 (9H, s).

To a stirred solution of (S)-1-[7-[(*tert*-butyldiphenylsilyl)oxy]naphthalen-1-yl]-2-oxo-3-[(2-[1-(triphenylmethyl)-1*H*-imidazol-4-yl]ethyl)amino]pyrrolidine (1.20 g, 1.47 mmol) in degassed DMF (15 mL) was added di-*tert*-butyl dicarbonate (352 mg, 1.61 mmol), and the resulting mixture was stirred at ambient temperature for 18 h. The solvent was removed under reduced pressure and the residue was purified by flash column chromatography on silica, with elution by EtOAc/1% MeOH/0.1% NH₄OH, to yield the titled product (728 mg, 54%): ¹H NMR (CDCl₃) δ 7.76–7.62 (6H, m), 7.42–7.22 (16H, m), 7.20–7.05 (9H, m), 6.96 and 6.74 (1H, m), 6.66–6.60 (1H, m), 4.12–3.28 (4H, m), 3.20–2.98 (1H, m), 2.90–2.75 (2H, m), 2.27–2.10 (1H, m), 2.01 (1H, m), 1.42 (9H, s), 1.11 (9H, s); MS (ES) *m/z* = 917 (M⁺ + H).

(vi) **4-Cyano-3-fluorobenzyl Alcohol (63).** To a stirred solution of aldehyde **30** (620 mg, 4.16 mmol) in EtOH (30 mL) at 0 °C was added NaBH₄ (157 mg, 4.16 mmol) in one portion. The reaction mixture was stirred at 0 °C for 10 min, and then 10% aqueous citric acid (10 mL) was added and the solvent was removed under reduced pressure. The residue was partitioned between saturated aqueous NaHCO₃ (10 mL) and CH₂Cl₂ (30 mL). The aqueous layer was extracted further with CH₂Cl₂ (30 mL). The combined organic extracts were dried over MgSO₄, filtered, and concentrated in vacuo to provide the titled compound as a white solid (615 mg, 98%): ¹H NMR (CDCl₃) δ 7.61 (1H, dd, *J* = 7.8, 6.7 Hz), 7.27 (1H, m), 7.24 (1H, dd, *J* = 8.6, 0.7 Hz), 4.80 (2H, d, *J* = 5.6 Hz), 1.90 (1H, t, *J* = 5.8 Hz); MS (EI) *m/z* = 151 (M⁺); HPLC purity = 98.6% (method B, 215 nm).

(vii) **(S)-{1-[7-[(*tert*-Butyldiphenylsilyl)oxy]naphthalen-1-yl]-2-oxopyrrolidin-3-yl}-2-[3-(4-cyano-3-fluorobenzyl)-3*H*-imidazol-4-yl]ethyl} carbamic Acid *tert*-Butyl Ester (64).** By the procedure for compound **34** but with **62** in place of **33** and **63** in place of **31**, the titled compound was obtained as a pale foam (518 mg, 82%): ¹H NMR (CDCl₃) δ 7.79–7.68 (6H, m), 7.51–7.16 (11H, m), 6.95–6.56 (4H, m), 5.27–4.90 (2H, m), 4.38 and 3.93 (1H, m), 3.30–2.67 (6H, m), 2.50 and 2.20 (1H, m), 1.93 (1H, m), 1.47 (9H, s), 1.11 (9H, s); MS (ES) *m/z* = 808 (M⁺ + H); HPLC purity = 99.8% (method B, 215 nm).

(viii) **(20*S*)-19,20,22,23-Tetrahydro-19-oxo-5*H*,21*H*-18,20-ethano-12,14-etheno-6,10-methenobenz[*d*]imidazo[4,3-*f*][1,6,9,13]oxatriazacyclononadecosine-9-carbonitrile Hydrochloride (66).** To a stirred solution of silyl ether **64** (1.30 g, 1.61 mmol) in THF (15 mL) was added TBAF (1 M in THF, 1.77 mL, 1.77 mmol), dropwise. The mixture was stirred at

ambient temperature for 30 min and then concentrated in vacuo. The residue was purified by flash column chromatography on silica, with elution by $\text{CHCl}_3/2\%$ $\text{MeOH}/0.2\%$ NH_4OH , to yield (S)-[2-[3-(4-cyano-3-fluorobenzyl)-3H-imidazol-4-yl]ethyl]-[1-[7-hydroxynaphthalen-1-yl]-2-oxopyrrolidin-3-yl]carbamic acid *tert*-butyl ester as a white foam (870 mg, 95%): ^1H NMR (CDCl_3) δ 7.76 (1H, d, $J = 9.0$ Hz), 7.71 (1H, d, $J = 8.3$ Hz), 7.57 (1H, dd, $J = 7.7, 6.9$ Hz), 7.43 (1H, s), 7.29–7.13 (5H, m), 6.94 (1H, d, $J = 7.9$ Hz), 6.84 (1H, d, $J = 9.2$ Hz), 6.14 (1H, br s), 5.27 (2H, s), 4.13 (1H, m), 3.88 (1H, m), 3.68 (1H, t, $J = 9.4$ Hz), 3.49 (1H, m), 3.13–2.96 (2H, m), 2.74 (1H, m), 2.54 (1H, m), 2.31 (1H, m), 1.49 (9H, s); HPLC purity = 100% (method B, 215 nm).

A mixture of (S)-[2-[3-(4-cyano-3-fluorobenzyl)-3H-imidazol-4-yl]ethyl]-[1-[7-hydroxynaphthalen-1-yl]-2-oxopyrrolidin-3-yl]carbamic acid *tert*-butyl ester (870 mg, 1.53 mmol) and Cs_2CO_3 (1.15 g, 3.53 mmol) in dry, degassed DMF (300 mL) was stirred at 45 °C for 18 h. Acetic acid (0.06 mL, 1.0 mmol) was added and the solvent was removed under reduced pressure. The residue was purified by flash column chromatography on silica, with elution by $\text{CHCl}_3/2\%$ $\text{MeOH}/0.2\%$ NH_4OH , to yield (20S)-21-(*tert*-butoxycarbonyl)-19,20,22,23-tetrahydro-19-oxo-5*H*,21*H*-18,20-ethano-12,14-etheno-6,10-methenobenz[*d*]imidazo[4,3-*l*][1,6,9,13]oxatriazacyclononadecosine-9-carbonitrile (**65**), which was dissolved in EtOAc (20 mL), cooled to 0 °C, and then saturated with HCl (g). After standing at 0 °C for 15 min, the mixture was concentrated to dryness under reduced pressure to yield the titled product as a white solid (627 mg, 79%): ^1H NMR (CD_3OD) δ 9.19 (1H, d, $J = 1.3$ Hz), 8.13 (1H, d, $J = 9.0$ Hz), 8.01 (1H, d, $J = 7.5$ Hz), 7.79 (1H, d, $J = 8.1$ Hz), 7.72 (1H, s), 7.66–7.55 (4H, m), 7.53 (1H, dd, $J = 9.0, 2.4$ Hz), 6.65 (1H, br s), 5.68–5.40 (2H, m), 4.63 (1H, m), 4.28–3.19 (4H, m), 3.20–2.97 (2H, m), 2.79 (1H, m), 2.42 (1H, m); MS (ES) $m/z = 450$ ($\text{M}^+ + \text{H}$); HPLC purity = 99.8% (method B, 215 nm); e.e. = 98.9%; Anal. ($\text{C}_{27}\text{H}_{23}\text{N}_5\text{O}_2 \cdot 1.9\text{HCl} \cdot 0.8\text{H}_2\text{O} \cdot 0.4\text{EtOAc}$) C, H, N.

Synthesis of (17*R*, 20*R*)-19,20,21,22-Tetrahydro-19-oxo-17*H*-15,17,18,20-diethano-6,10,12,16-dimetheno-16*H*-imidazo[3,4-*h*][1,8,11,14]oxatriazacycloeicosine-9-carbonitrile Hydrochloride (78**):** (i) 6-[(*tert*-Butyldiphenylsilyl)oxy]-1-indanol (**71**). A mixture of 6-hydroxy-1-indanone²² (**70**) (5.00 g, 33.8 mmol), *tert*-butyldiphenylsilyl chloride (23.1 g, 84.2 mmol), and imidazole (6.90 g, 101.4 mmol) in degassed DMF (100 mL) was heated at 60 °C for 18 h. The solvent was removed in vacuo and the residue was purified by silica gel chromatography, with elution by hexane/10% EtOAc, to yield 6-[(*tert*-butyldiphenylsilyl)oxy]-1-indanone as an oil (12.8 g, 98%): ^1H NMR (CDCl_3) δ 7.69 (4H, d, $J = 7.9$ Hz), 7.43–7.33 (6H, m), 7.17–7.13 (2H, m), 6.96 (1H, dd, $J = 8.3, 2.4$ Hz), 3.01–2.96 (2H, m), 2.66–2.61 (2H, m), 1.10 (9H, s).

To a solution of 6-[(*tert*-butyldiphenylsilyl)oxy]-1-indanone (12.6 g, 32.6 mmol) in MeOH (500 mL) was added NaNH_4 (3.2 g, 84.6 mmol), portionwise, over 5 min. The resulting mixture was stirred at ambient temperature for 1 h and then cooled to 0 °C. The chilled solution was adjusted to pH = 4.5 with dilute aqueous HCl, and most of the MeOH was removed under reduced pressure. The residue was partitioned between saturated aqueous NaHCO_3 (75 mL) and CHCl_3 (150 mL). The organic layer was removed, and the aqueous phase was extracted further with CHCl_3 (2×100 mL). The combined organic extracts were washed with brine, then dried over MgSO_4 , filtered, and concentrated in vacuo. The residue was purified by silica gel chromatography, with elution by hexane/10% EtOAc, to yield the titled product as a colorless oil (10.3 g, 81%): ^1H NMR (CDCl_3) δ 7.72 (4H, d, $J = 7.7$ Hz), 7.45–7.33 (6H, m), 6.92 (1H, d, $J = 8.2$ Hz), 6.82 (1H, d, $J = 2.2$ Hz), 6.63 (1H, dd, $J = 8.2, 2.3$ Hz), 5.06 (1H, td, $J = 6.8, 5.7$ Hz), 2.90 (1H, ddd, $J = 15.5, 8.5, 4.8$ Hz), 2.67 (1H, m), 2.42 (1H, m), 1.88 (1H, m), 1.48 (1H, d, $J = 7.1$ Hz), 1.10 (9H, s).

(ii) 6-[(*tert*-Butyldiphenylsilyl)oxy]-1-indanyl Azide (**72**). By the procedure for compound **5** but with **71** in place of **4**, the titled product was obtained as a colorless oil (6.10 g,

99%): ^1H NMR (CDCl_3) δ 7.74–7.69 (4H, m), 7.45–7.34 (6H, m), 6.95 (1H, d, $J = 8.2$ Hz), 6.80 (1H, d, $J = 2.4$ Hz), 6.67 (1H, dd, $J = 8.2, 2.4$ Hz), 4.63 (1H, dd, $J = 7.1, 4.8$ Hz), 2.92 (1H, m), 2.72 (1H, m), 2.38 (1H, m), 2.06 (1H, m), 1.10 (9H, s).

(iii) 6-[(*tert*-Butyldiphenylsilyl)oxy]-1-indanylamine (**73**). By the procedure for compound **6** but with **72** in place of **5**, the titled compound was obtained as an oil (3.40 g, 59%): ^1H NMR (CDCl_3) δ 7.74–7.68 (4H, m), 7.45–7.33 (6H, m), 6.89 (1H, d, $J = 8.1$ Hz), 6.70 (1H, d, $J = 2.1$ Hz), 6.57 (1H, dd, $J = 8.1, 2.4$ Hz), 4.17 (1H, t, $J = 7.5$ Hz), 2.79 (1H, ddd, $J = 15.4, 8.6, 3.2$ Hz), 2.65 (1H, m), 2.42 (1H, m), 2.06 (1H, ddt, $J = 12.6, 7.9, 8.6$ Hz), 1.46 (2H, br s), 1.10 (9H, s).

(iv) (2*R*)-2-[(*tert*-Butoxycarbonyl)amino]-4-(methylmercapto)-*N*-[6-[(*tert*-butyldiphenylsilyl)oxy]indan-1-yl]-butyramide, Diastereomers A and B (**74**). By the procedure for compound **7** but with **73** in place of **6**, the titled compounds were obtained as a mixture of diastereomers (2.30 g, 85%): ^1H NMR (CDCl_3) δ 7.74–7.66 (4H, m), 7.46–7.33 (6H, m), 6.92–6.86 (1H, m), 6.71 (1H, one isomer, br s), 6.64 (1H, one isomer, br s), 6.61–6.72 (1H, m), 6.20–6.09 (1H, m), 5.34–5.25 (1H, m), 5.15 (1H, one isomer, br d), 5.06 (1H, one isomer, br d), 4.25–4.13 (1H, m), 2.87–2.78 (1H, m), 2.75–2.66 (1H, m), 2.60–2.44 (3H, m), 2.14–2.00 (1H, m), 2.11 (3H, one isomer, s), 2.07 (3H, one isomer, s), 1.95–1.82 (1H, m), 1.80–1.66 (1H, m), 1.46 (9H, one isomer, s), 1.44 (9H, one isomer, s), 1.09 (9H, one isomer, s), 1.08 (9H, one isomer, s).

(v) (3*R*)-3-[(*tert*-Butoxycarbonyl)amino]-1-[6-[(*tert*-butyldiphenylsilyl)oxy]indan-1-yl]-2-oxopyrrolidine, Diastereomers A and B (**75** and **76**). By the procedures for compound **8** but with **74** in place of **7**, the titled compounds were obtained. The diastereomers were separated by flash column chromatography on silica, with elution by a gradient of hexane/20–35% EtOAc, to yield the titled compounds, diastereomer A (**75**) (the isomer of higher R_f) (872 mg, 42%) and diastereomer B (**76**) (the isomer of lower R_f) (820 mg, 39%): ^1H NMR (CDCl_3) δ 7.74–7.64 (4H, m), 7.47–7.31 (6H, m), 6.99 (1H, d, $J = 8.4$ Hz), 6.75 (1H, dd, $J = 8.2, 2.3$ Hz), 6.36 (1H, d, $J = 1.9$ Hz), 5.54 (1H, t, $J = 7.8$ Hz), 5.00 (1H, br s), 4.13 (1H, m), 2.96 (1H, td, $J = 10.1, 6.3$ Hz), 2.86–2.71 (2H, m), 2.59 (1H, t, $J = 9.3$ Hz), 2.46 (1H, m), 2.30 (1H, dtd, $J = 12.9, 8.1, 4.2$ Hz), 1.82 (1H, m), 1.49 (9H, s), 1.30 (1H, m), 1.08 (9H, s).

(vi) (*R,R*)-4-{[5-([1-(6-Hydroxyindan-1-yl)-2-oxopyrrolidin-3-yl]amino)methyl]imidazol-1-yl]methyl}-2-fluorobenzonitrile (**77**). Pyrrolidinone **76** (the *R,R* isomer), (270 mg, 0.47 mmol) was dissolved in CH_2Cl_2 (5 mL), and TFA (0.72 mL, 9.4 mmol) was added dropwise. The resulting mixture was stirred at ambient temperature for 18 h and then concentrated under reduced pressure to afford (*R,R*)-3-amino-1-[6-[(*tert*-butyldiphenylsilyl)oxy]indan-1-yl]-2-oxopyrrolidine trifluoroacetate as a white foam (275 mg, 99%): ^1H NMR (CD_3OD) δ 7.73 (2H, m), 7.67 (2H, m), 7.49–7.33 (6H, m), 7.03 (1H, d, $J = 8.2$ Hz), 6.73 (1H, dd, $J = 8.2, 2.2$ Hz), 6.49 (1H, d, $J = 1.9$ Hz), 5.49 (1H, t, $J = 7.7$ Hz), 4.00 (1H, dd, $J = 11.2, 8.4$ Hz), 2.96 (1H, td, $J = 9.9, 6.3$ Hz), 2.88 (1H, ddd, $J = 15.8, 9.0, 4.0$ Hz), 2.78 (1H, m), 2.65 (1H, t, $J = 9.4$ Hz), 2.43–2.27 (2H, m), 2.30 (1H, ddt, $J = 13.1, 8.6, 7.7$ Hz), 1.59 (1H, m), 1.07 (9H, s).

(*R,R*)-3-Amino-1-[6-[(*tert*-butyldiphenylsilyl)oxy]indan-1-yl]-2-oxopyrrolidine trifluoroacetate (170 mg, 0.29 mmol) and 1-(4-cyano-3-fluorobenzyl)-5-imidazolecarboxaldehyde (60 mg, 0.26 mmol) were stirred in MeOH (3 mL) for 30 min at ambient temperature, and then NaCNBH_3 (22 mg, 0.35 mmol) was added and stirring was continued for 18 h. The solvent was evaporated and the residue was dissolved in THF (5 mL). To this solution was added TBAF (1.0 M in THF, 0.34 mL, 0.34 mmol); stirring was continued for 15 min, and then the solvent was evaporated. The residue was partitioned between saturated aqueous NaHCO_3 (5 mL) and CHCl_3 (10 mL). The aqueous layer was extracted further with CHCl_3 (2×5 mL). The combined organic extracts were dried over MgSO_4 , filtered, and concentrated in vacuo. The crude product was purified by flash column chromatography on silica, with elution by $\text{CHCl}_3/5\%$ $\text{MeOH}/0.5\%$ NH_4OH , to yield the titled product as a

colorless oil (97 mg, 75%): ^1H NMR (CDCl_3) δ 7.60 (1H, dd, J = 7.8, 6.7 Hz), 7.57 (1H, s), 7.07 (1H, d, J = 8.1 Hz), 7.02 (1H, d, J = 8.3 Hz), 7.00 (1H, s), 6.95 (1H, d, J = 9.6 Hz), 6.75 (1H, dd, J = 8.1, 2.1 Hz), 6.35 (1H, d, J = 1.7 Hz), 5.61 (1H, m), 5.60 (1H, d, J = 16.8 Hz), 5.41 (1H, d, J = 16.8 Hz), 3.80 (1H, d, J = 14.1 Hz), 3.73 (1H, d, J = 14.2 Hz), 3.52 (1H, dd, J = 9.8, 8.2 Hz), 3.13 (1H, td, J = 9.4, 7.0 Hz), 2.95–2.76 (3H, m), 2.34 (1H, m), 2.10 (1H, m), 1.93 (1H, ddt, J = 13.1, 8.2, 7.8 Hz), 1.65 (1H, m).

(vii) (17R, 20R)-19,20,21,22-Tetrahydro-19-oxo-17H-15,17:18,20-diethano-6,10:12,16-dimetheno-16H-imidazo[3,4-h][1,8,11,14]oxatriazacycloecosine-9-carbonitrile Hydrochloride (78). A mixture of phenol **77** (97 mg, 0.22 mmol) and Cs_2CO_3 (142 mg, 0.44 mmol) in dry, degassed DMF (40 mL) was stirred at 50 °C under argon for 1 h. The solvent was removed under reduced pressure, and the residue was partitioned between saturated aqueous NaHCO_3 (1 mL) and CHCl_3 (3 mL). The aqueous layer was extracted further with CHCl_3 (2 \times 3 mL). The combined organic extracts were dried over MgSO_4 , filtered, and concentrated in vacuo. The crude product was purified by flash column chromatography on silica, with elution by CHCl_3 /6% MeOH/0.6% NH_4OH , to yield the desired product, which was converted to the hydrochloride salt by treatment with HCl in EtOAc (105 mg, 97%): ^1H NMR (CD_3OD) δ 9.44 (1H, d, J = 1.2 Hz), 7.82 (1H, d, J = 7.9 Hz), 7.66 (1H, s), 7.45 (1H, s), 7.42 (1H, d, J = 8.2 Hz), 7.25 (1H, dd, J = 8.2, 2.4 Hz), 7.18 (1H, dd, J = 7.9, 1.2 Hz), 6.83 (1H, d, J = 2.1 Hz), 5.70 (1H, d, J = 15.6 Hz), 5.63 (1H, dd, J = 8.9, 3.1 Hz), 5.53 (1H, d, J = 15.6 Hz), 4.56 (1H, dd, J = 9.6, 8.4 Hz), 4.31 (1H, d, J = 14.3 Hz), 3.81 (1H, dd, J = 14.3, 0.9 Hz), 3.64 (1H, m), 3.27 (1H, m), 3.15 (1H, m), 3.02 (1H, ddd, J = 16.2, 9.3, 3.8 Hz), 2.62–2.33 (3H, m), 2.27 (1H, m); MS (ES) m/z = 426 (M^+ + H); HPLC purity = 99.6% (method B, 215 nm); Anal. ($\text{C}_{25}\text{H}_{23}\text{N}_5\text{O}_2 \cdot 2\text{HCl} \cdot \text{H}_2\text{O} \cdot 0.2\text{EtOAc}$) C, H, N.

Acknowledgment. We thank Kenneth D. Anderson, Patrice A. Ciecko-Steck, Graham M. Smith, Bang-Lin Wan, and Matthew M. Zrada for analytical chemistry support; Arthur B. Coddington, Harri G. Ramjit, and Charles W. Ross III for mass spectral analyses; Joan S. Murphy, Steven M. Pitzenberger, and Sandor L. Varga for NMR spectroscopy expertise; Neville Anthony for critical reading of the manuscript; and Margaret Guttman for manuscript preparation.

Supporting Information Available: Characterization data for all final compounds that are not described in the Experimental Section of this paper, X-ray crystallography diffraction data and refinement statistics. This information is available free of charge via the Internet at <http://pubs.acs.org>.

References

- Casey, P. J.; Soliski, P. A.; Der, C.; Buss, J. E. p21 Ras is Modified by a Farnesyl Isoprenoid. *Proc. Natl. Acad. Sci. U.S.A.* **1989**, *86*, 8323–8327.
- Willumsen, B. M.; Norris, K.; Papageorge, A. G.; Hubbert, N. L.; Lowy, D. R. Harvey Murine Sarcoma Virus p21 Ras Protein: Biological and Biochemical Significance of the Cysteine Nearest the Carboxy Terminus. *EMBO J.* **1984**, *3*, 2581–2585.
- Bell, I. M. Inhibitors of Protein Prenylation 2000. *Exp. Opin. Ther. Patents* **2000**, *10*, 1813–1831.
- Oliff, A. Farnesyltransferase Inhibitors: Targeting the Molecular Basis of Cancer. *Biochim. Biophys. Acta* **1999**, *1423*, C19–C30.
- Williams, T. M. Inhibitors of Protein Prenylation 1999. *Exp. Opin. Ther. Patents* **1999**, *9*, 1263–1280.
- Bell, I. M.; Gallicchio, S. N.; Abrams, M.; Beshore, D. C.; Buser, C. A.; et al. Design and Biological Activity of (S)-4-(5-([1-(3-Chlorobenzyl)-2-oxopyrrolidin-3-ylamino]methyl)imidazol-1-yl-methyl)benzonitrile, a 3-Aminopyrrolidinone Farnesyltransferase Inhibitor with Excellent Cell Potency. *J. Med. Chem.* **2001**, *44*, 2933–2949.
- Dinsmore, C. J.; Bogusky, M. J.; Culbertson, J. C.; Bergman, J. M.; Homnick, C. F.; et al. Conformational Restriction of Flexible Ligands Guided by the Transferred NOE Experiment: Potent Macrocyclic Inhibitors of Farnesyltransferase. *J. Am. Chem. Soc.* **2001**, *123*, 2107–2108.
- Anthony, N. J.; Gomez, R. P.; Schaber, M. D.; Mosser, S. D.; Hamilton, K. A.; et al. Design and In Vivo Analysis of Potent Non-Thiol Inhibitors of Farnesyl Protein Transferase. *J. Med. Chem.* **1999**, *42*, 3356–3368.
- Mathre, D. J.; Thompson, A. S.; Douglas, A. W.; Hoogsteen, K.; Carroll, J. D.; et al. A Practical Process for the Preparation of Tetrahydro-1-methyl-3,3-diphenyl-1H,3H-pyrrolo[1,2-c][1,3,2]-oxazaborole-Borane, A Highly Enantioselective Stoichiometric and Catalytic Reducing Agent. *J. Org. Chem.* **1993**, *58*, 2880–2888.
- Kearsley, S. Merck & Co., Inc.
- Mohamadi, F.; Richards, N. G. J.; Guida, W. C.; Liskamp, R.; Lipton, M.; et al. MacroModel – An Integrated Software System for Modeling Organic and Bioorganic Molecules Using Molecular Mechanics. *J. Comput. Chem.* **1990**, *11*, 440–467.
- Otwinowski, Z.; Minor, W. Processing of X-ray Diffraction Data Collected in Oscillation Mode. *Methods Enzymol.* **1997**, *276A*, 307–326.
- Long, S. B.; Hancock, P. J.; Kral, A. M.; Hellinga, H. W.; Beese, L. S. The Crystal Structure of Human Protein Farnesyltransferase Reveals the Structural Basis for Inhibition by CaaX Tetrapeptides and their Mimetics. *Proc. Natl. Acad. Sci. U.S.A.* **2001**, *98*, 12948–12953.
- Jones, T. A.; Kjeldgaard, M. *O Version 5.9, The Manual*; Uppsala University: Uppsala, Sweden, 1993.
- Brunger, A. T.; Adams, P. D.; Clore, G. M.; DeLano, W. L.; Gros, P.; et al. Crystallography & NMR System: A New Software Suite for Macromolecular Structure Determination. *Acta Crystallogr., Sect. D* **1998**, *54*, 905–921.
- Bellamy, W. T. P-Glycoproteins and Multidrug Resistance. *Annu. Rev. Pharmacol. Toxicol.* **1996**, *36*, 161–183.
- Long, S. B.; Casey, P. J.; Beese, L. S. The Basis for K-Ras4B Binding Specificity to Protein Farnesyltransferase Revealed By 2 Å Resolution Ternary Complex Structures. *Structure* **2000**, *8*, 209–222.
- Burley, S. K.; Petsko, G. A. Weakly Polar Interactions in Proteins. *Adv. Protein Chem.* **1988**, *39*, 125–192.
- Hunter, C. A.; Sanders, J. K. M. The Nature of π - π Interactions. *J. Am. Chem. Soc.* **1990**, *112*, 5525–5534.
- Hunter, C. A.; Singh, J.; Thornton, J. M. π - π Interactions: the Geometry and Energetics of Phenylalanine–Phenylalanine Interactions in Proteins. *J. Mol. Biol.* **1991**, *218*, 837–846.
- Williams, T. M.; Bergman, J. M.; Brashear, K.; Breslin, M. J.; Dinsmore, C. J.; et al. N-Arylpiperazinone Inhibitors of Farnesyltransferase: Discovery and Biological Activity. *J. Med. Chem.* **1999**, *42*, 3779–3784.
- Nayak, M. K.; Chakraborti, A. K. Chemoselective Aryl Alkyl Ether Cleavage by Thiophenolate Anion Through Its In Situ Generation in Catalytic Amount. *Tetrahedron Lett.* **1997**, *38*, 8749–8752.

JM010531D